UNIVERSITY OF TARTU

FACULTY OF SCIENCE AND TECHNOLOGY

INSTITUTE OF MOLECULAR AND CELL BIOLOGY

INSTITUTE OF TECHNOLOGY

Characterization of plasma membrane proton pump AHA1 mutants

Master's Thesis

30 ECTS

Jaanika Unt

Supervisors

Dr. Dmitry Yarmolinsky

Prof. Hannes Kollist

Tartu, 2020

UNIVERSITY OF TARTU

ABSTRACT

Characterization of plasma membrane proton pump AHA1 mutants

The gas exchange of plants is regulated by microscopic pores, stomata. Each stoma consists of two specialized guard cells and a pore that can be closed or open according to prevailing environmental conditions. For the stomatal opening, various ions and water need to accumulate in the guard cells. The entry of these osmolytes is driven by energy produced by the plasma membrane proton pump AHA1, which is considered as the main proton pump in stomata of *Arabidopsis thaliana*. The role of AHA1 in guard cells has been studied for a long time, although its regulation and functioning are not completely understood. The aim of this Master's thesis was to study newly-identified mutations in AHA1, which could clarify some of these aspects. Experiments with the AHA1 backcrossed mutant lines and generated transgenic plants corresponding to some of these mutations bring structural insight for the AHA1 regulation and highlight its importance for CO_2-induced stomatal movements.

Keywords: stomata, guard cells, gas exchange, proton pump

CERCS: B310 Physiology of vascular plants

Plasmamembraani prootonpumba AHA1 mutantide analüüs

Taimede gaasivahetuse eest vastutavad vartel ja lehtedel paiknevad kahest sulgrakust koosnevad poorid, mida kutsutakse õhulõhedeks. Turgorrõhu muutused sulgrakkudes reguleerivad õhulõhede avatust erinevatele keskkonnatingimustele. Õhulõhede avanemisreaktsioonil kogunevad sulgrakkudesse mitmed ioonid ja vesi, mille sisenemine on tagatud plasmamembraani prootonpumpade poolt tekitatud energia arvelt. Taimebioloogia mudelorganismi hariliku müürlooga sulgrakkudes on keskseks prootonpumbaks AHA1. Antud prootonpumba rolli õhulõhedes on kaua uuritud, kuid jätkuvalt on lünkasid AHA1 regulatsiooni ja tööpõhimõtete mõistmisel. Käesoleva magistritöö raames uuriti uusi AHA1 mutatsiooniga taimeliine. Eksperimendid antud liinide ja loodud transgeensete taimedega annavad uut informatsiooni AHA1 prootonpumba regulatsiooni kohta ja näitavad AHA1 rolli CO_2-toimelise õhulõhede sulgumisel.

Märksõnad: õhulõhed, sulgrakud, gaasivahetus, prootonpump

CERCS: B310 soontaimede füsioloogia

TABLE OF CONTENTS

ABBREVIATIONS

ABA – abscisic acid

ABA4 – ABSCISIC ACID DEFICIENT 4

ABCB14 – ATP-BINDING CASSETTE B14

ABI1; ABI2 – ABA INSENSITIVE 1; 2

A-domain – actuator domain

AHA – ARABIDOPSIS THALIANA H^+-ATPASE

AKT1 – ARABIDOPSIS THALIANA K^+ TRANSPORTER 1

ALMT – ALUMINUM-ACTIVATED MALATE TRANSPORTERS

CAPS – cleaved amplified polymorphic sequence

cDNA – complementary DNA

CLSM – confocal laser scanning microscopy

CPK – CALCIUM-DEPENDENT PROTEIN KINASES

EMS – ethyl methanesulfonate

GHR1 – GUARD CELL HYDROGEN PEROXIDE-RESISTANT 1

GORK – GATED OUTWARDLY-RECTIFYING K^+ CHANNELS

HT1 – HIGH LEAF TEMPERATURE 1

KAT1; KAT2 – POTASSIUM CHANNEL IN ARABIDOPSIS THALIANA 1; 2

L*er* – Landsberg *erecta*

M-domain – transmembrane domain

MPK4; MPK12 – MITOGEN-ACTIVATED PROTEIN KINASES 4; 12

N-domain – nucleotide-binding domain

NRT1.1 – NITRATE TRANSPORTER 1

OST1; OST2 – OPEN STOMATA 1; 2

P-domain – phosphorylation domain

PIP2;1 – PLASMEMBRANE INTRINSIC PROTEIN 2;1

Pma1 – PLASMA MEMBRANE ATPASE 1

PP2C – TYPE-2C PROTEIN PHOSPHATASE

ppm – parts per million

PYR/PYL/RCAR – PYRABACTIN RESISTANCE 1/PYR1- LIKE/REGULATORY COMPONENTS OF ABA RECEPTORS

QUAC1 – QUICK-ACTIVATING ANION CHANNEL 1

R-domain – regulatory domain

ROS – reactive oxygen species

SLAC1 – SLOW ANION CHANNEL ASSOCIATED 1

SLAH3 – SLAC1 HOMOLOGUE 3

SnRK2 – SUCROSE NONFERMENTING 1-RELATED SUBFAMILY 2 KINASES

T-DNA – transfer DNA

WT – wild-type

YC3.6 – yellow cameleon construct 3.6

βCA1; βCA4 – BETA CARBONIC ANHYDRASE1; 4

INTRODUCTION

The sessile life cycle has forced plants to evolve specific mechanisms to rapidly react towards ever-changing environmental conditions on land. Plants have to continuously adapt to fluctuating light, temperature, and rainfall patterns as well as exposure to air pollutants and pathogen attacks. The gas-exchange between a plant and the atmosphere is controlled by small pores on aerial green surfaces, which are called stomata. Plants require the uptake of CO_2 from the air for photosynthesis and building the biomass, although this process is accompanied water evaporation from leaves. The function of stomata is to regulate the unavoidable trade-off between these processes and to ensure optimal conditions for photosynthesis and plant growth.

The concentration of atmospheric CO_2 has been steadily rising since the beginning of the industrial revolution. It influences the Earth climate by causing the greenhouse effect and affects plant growth and development. The climate change has also led to more frequent extreme weather conditions, such as risen temperatures and long-lasting droughts (IPCC, 2014). The declining water supplies in agriculturally important regions have become the biggest limit for crop productions (Lesk et al., 2016). To provide the food security for the growing global population, more elaborative approaches in agriculture are needed. One of the current trends is to increase crop productivity by breeding plants with improved water use efficiency. As stomatal pores control water evaporation and CO_2 uptake, studies of stomatal regulation can provide a solution for this.

Crop plants can be difficult objects for studies in laboratories. For this reason, *Arabidopsis thaliana*, also known as the thale cress, is widely used as a model organism in modern plant physiology. Although it does not have an agronomic significance, due to its compact size, the relatively small diploid genome, a rapid life cycle and a vast amount of genetic resources, *Arabidopsis* offers substantial scientific advantages to acquire generic knowledge about plant form and function.

The function of plasma membrane proton pump AHA1 is known to drive stomatal opening. The purpose of this Master's thesis was to characterize novel *Arabidopsis* AHA1 mutants isolated in the large-scale screen. The current study was performed in The Plant Signal Research Group at the Institute of Technology.

1. LITERATURE REVIEW

1.1. Importance of stomata

Plants require atmospheric CO_2 for photosynthesis that produces energy and assimilates carbon while oxygen is released as a by-product. At the same time, plants should control transpiration, the water movement through a plant and its evaporation from leaves. The gas-exchange between the interior tissues of plants and the atmosphere is regulated by minuscule pores, stomata. Since relative air humidity inside a leaf is close to 100% and significantly lower in the surrounding environment, water vapour diffusion out from the leaf happens simultaneously with CO_2 uptake. Therefore, plants need an optimal trade-off between these crucial events for growth and survival.

Stomata can be found on the surfaces of leaves and stalks. In plant model organism *Arabidopsis thaliana,* stomata are mainly located on the lower sides of the leaves (Willmer and Ficker, 1996). It helps the plants to keep stomata out of the direct sunlight to prevent excessive water loss. Stomata are formed by pairs of specialized guard cells and an orifice between them (Fig. 1). Guard cells control opening and closure of a pore which they form. Stomatal aperture depends on swelling or shrinking of guard cells which are able to change their turgor pressure and volume (Waggoner and Zelitch, 1965). An increase in the turgor pressure of guard cells results in stomatal opening and activation of gas exchange processes. A loss of the turgor pressure makes guard cells flaccid, leading to stomatal closure.

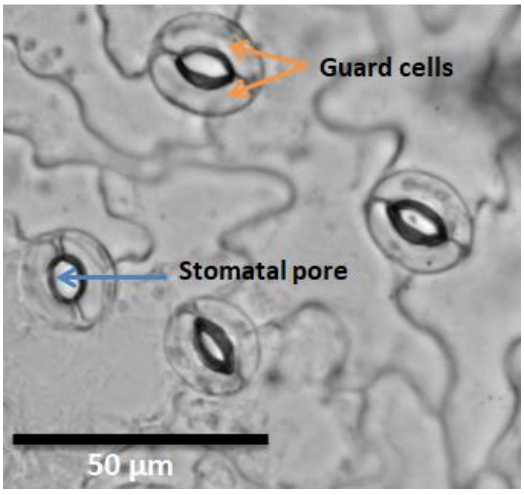

Figure 1. Open stomata of *A.thaliana* wildtype Col-0 line under a light microscope. The epidermis of a leaf has been peeled off and incubated in liquid a buffer with KCl under a light source. The brightfield picture shows stomata composed of two specialized guard cells and the stomatal pore between them.

Numerous experiments have demonstrated that stomatal apertures are influenced by a variety of environmental factors, including atmospheric CO_2 concentrations, light intensity, air temperature, and photoperiod (Kollist et al., 2014). Internal mediators also play important roles in the regulation of stomatal apertures. Thus, the plant hormone abscisic acid (ABA) is considered as one of the key phytohormones in stomatal regulation. Notably, stomatal opening and closure are frequently triggered by the opposing factors For instance, high concentrations of CO_2 induce stomatal closure while its low concentrations trigger stomatal opening, similarly reduced air humidity leads to stomatal closure whereas high humidity promotes stomatal opening. It should be noted that open stomata are also points of entry for toxic gases and pathogens. The ground-level ozone is considered to be one of the most damaging air pollutants as it oxidizes the inner tissues of plants (Hopkin, 2007; Ainsworth et al., 2012). Taken together, stomata play a role of an interface that mediates plant interactions with the surrounding environment and, thus, research of mechanisms that control stomatal movements is important for understanding how plants adapt to ever-changing environmental conditions.

1.2. Stomatal movements

The fluctuations of various environmental and endogenous stimuli are converted into signals inside guard cells that control stomatal movements through multiple interconnected pathways. Regulating apertures of stomata involves dynamic adjustments of osmotic pressure in guard cells (Fig. 2) (Roelfsema and Hedrich, 2005). The turgor pressure is increased when osmolytes and ions (mostly, K^+ and NO_3^-, Cl^- and $malate^{2-}$) are accumulated in guard cells. This leads to a temporal decline in water potential, which induces water inflow. As turgor pressure elevates, guard cells swell and due to their specific anatomic features bend to widen the distance between them, opening the stomatal pore. Stomatal closure reverses these processes and decreases the turgor and osmotic pressure in guard cells. The movements of solutes during both stomatal opening and closure are directed by ion channels, transporters, and pumps in guard cell membranes (Daszkowska-Golec and Szarejko, 2013). A large number of molecular studies have revealed many components of signalling pathways in guard cells, although several aspects of stomatal regulation remain unknown.

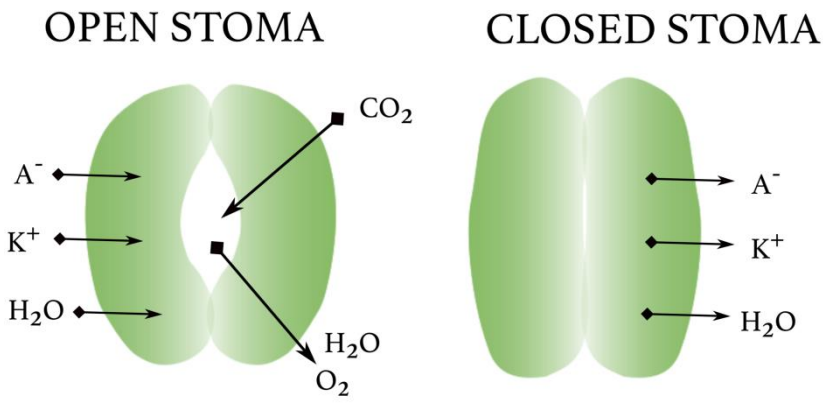

Figure 2. A simplified scheme of stomatal movements. Stomatal opening and closure are caused by transportation of anions (A^-), potassium (K^+) as well as water inflow or outflow. Through an open stoma, water vapor and oxygen are released and carbon dioxide enters.

1.2.1. Stomatal opening

It has been well-established that one of the fundamental components of stomatal opening mechanism is activity of ATP-driven proton pumps (H^+-ATPases) in guard cells. Functioning of these pumps is known to be altered in response to many environmental stimuli. For example, illumination is considered as one of the main factors that positively regulates H^+-ATPases in guard cells (Shimazaki et al., 2007).

Light-induced stomatal opening can be triggered by blue and red light, although blue light is considered to be more effective in the stimulation of this process (Sharkey and Raschke, 1981). Blue and red light induce stomatal opening through two different signalling pathways that both stimulate H^+-ATPases. The activation of H^+-ATPase requires phosphorylation of C-terminus and is, in some cases, followed by the binding of a 14-3-3 protein (Kinoshita and Shimazaki 2002). Plasma membrane H^+-ATPases utilize energy from the hydrolysis of ATP to translocate protons from guard cell cytoplasm to apoplast. Transportation of protons creates two types of gradients that energize solute transport (Haruta et al., 2015). The efflux of protons generates electrical potential across the plasma membrane. Thereby, the membrane hyperpolarization leads to activation of voltage-dependent K^+ inward rectifying channels KAT1, KAT2 (POTASSIUM CHANNEL IN ARABIDOPSIS THALIANA 1; 2), and AKT1 (ARABIDOPSIS THALIANA K^+ TRANSPORTER 1) (Schachtman et al., 1992; Pilot et al., 2001; Szyroki et al., 2001). Additionally, the transmembrane chemical gradient emerges due to different proton concentrations inside and outside of guard cells. Furthermore, apoplastic acidification allows some solutes to penetrate into guard cells via concomitant uptake of protons (Palmgren, 2001). Anion influx balances positively charged K^+ and consequently,

maintains negative electrical potential (Sze, 1985). Inorganic NO_3^- and Cl^- are taken up by guard cells via symporters. So far, only a NO_3^- cotransporter has been discovered – NRT1.1 (NITRATE TRANSPORTER 1) (Guo et al., 2003). Additionally, organic malate^{2-} contributes to the solute pool in guard cell. In guard cells, malate can be released by the cytosolic breakdown of starch or taken up from apoplast by ABCB14 protein (ATP-BINDING CASSETTE B14) (Leet et al., 2008).

Accumulation of osmotically active ions drives water to move inward until water potential has been equilibrated on both sides of the plasma membrane. To facilitate the water movement, integral proteins called aquaporins are present in the plasma membrane of guard cells. Increased concentrations of ions, together with water, creates the turgor pressure that drives stomatal opening (Daszkowska-Golec and Szarejko, 2013).

1.2.2. Stomatal closure

During stomatal closure, H^+-ATPases are inhibited and anion channels responsible for anion efflux in guard cells are activated, leading to membrane depolarization (Roelfsema and Hedrich, 2005). Apparently, all recognized stomatal closure-triggering stimuli inhibit the activity of H^+-ATPases, including elevated CO_2 and ABA (Edwards and Bowling, 1985; Hayashi et al., 2011; Falhof et al., 2016). Multiple theories have been proposed to explain how environmental factors may down-regulate proton pumps during stomatal closure, but the underlying mechanisms are still not fully understood (Falhof et al., 2016).

Two types of anion channels have been reported to operate in guard cells: R-type and S-type anion channels that are activated rapidly and slowly, respectively, during stomatal closure (Schroeder and Keller, 1992). Besides the differences in the reaction time, R-type anion channels demonstrate a strong voltage dependency while currents through S-type channels only weakly correlate with voltage across the membrane.

Up to know, only QUAC1 (QUICK-ACTIVATING ANION CHANNEL 1), a member of ALMT (ALUMINUM-ACTIVATED MALATE TRANSPORTERS) family, has been identified as an R-type anion channel in the guard cell plasma membrane (Meyer et al., 2010). Mutants lacking functional QUAC1 have partially impaired responses to ABA, darkness, and elevated CO_2. The main S-type anion channel in guard cells is SLAC1 (SLOW ANION CHANNEL ASSOCIATED 1) (Negi et al., 2008; Vahisalu et al., 2008) that is closely related to another S-type channel

SLAH3 (SLAC1 HOMOLOGUE 3) (Geiger et al., 2011). Stomata of loss-of-function *slac1* mutants exhibit reduced responsiveness or complete insensitivity to the most endogenous and environmental stimuli, including ABA, CO_2 and ozone concentrations (Vahisalu et al., 2008). Overall, S- and R-type channels allow NO_3^-, Cl^-, and malate^{2-} efflux from guard cells (Negi et al. 2008; Geiger et al., 2011). These events result in K^+ outflow through gated outwardly-rectifying K^+ channels (GORK) (Ache et al., 2000). Water follows K^+ outflux, and guard cells shrink. Flaccid guard cells seal the stomatal pore, halting gas exchange in and out of a leaf.

1.2.3. ABA-induced stomatal closure

It was clearly demonstrated in the early 1970s that the plant hormone ABA is involved in promoting stomatal closure (Jones and Mansfield, 1970). At present, ABA is known to act as a key hormone regulating plant acclimation to drought, pathogen entry, salinity, cold, and UV radiation stress (Finkelstein, 2013). Even low concentrations (ca 1 µM) of the applied exogenous ABA are able to close stomata almost completely in isolated epidermises and partially in detached leaves (Trejo et al., 1993).

The signal transduction pathway of ABA has been revealed in many details (Fig. 3). In the absence of ABA, type-2C protein phosphatases (PP2Cs) keep SLAC1 anion channel in a dephosphorylated inactive state by inhibiting its positive regulators SnRK2.6/OST1 kinases (SUCROSE NONFERMENTING 1-RELATED SUBFAMILY 2 KINASES/OPEN STOMATA 1) and receptor-like protein GHR1 (GUARD CELL HYDROGEN PEROXIDE-RESISTANT 1) (Gosti et al., 1999; Fujii et al., 2009; Hua et al., 2012). Under stress conditions, accumulated ABA molecules in guard cells activate the cytoplasmic PYR/PYL/RCAR (PYRABACTIN RESISTANCE 1/PYR1- LIKE/REGULATORY COMPONENTS OF ABA RECEPTORS) ABA receptors (Ma et al., 2009; Park et al., 2009). These protein complexes are negative regulators of PP2Cs, including ABI1 and ABI2 (ABA INSENSITIVE 1 and 2) (Ma et al., 2009). The formation of the ternary complex between ABA, PP2Cs and PYR/PYL/RCARs inactivates attached PP2Cs and releases the OST1 kinase and GHR1 from inhibition by PP2C phosphatases (Umezawa et al., 2009; Hua et al., 2012). SnRK2s have been demonstrated to directly activate the SLAC1 anion channel (Geiger et al. 2009, Lee et al., 2009). A recent study shows that GHR1 is a pseudokinase, however, it is capable to promote activation of SLAC1 in *Xenopus* oocytes (Sierla et al., 2018). In addition, SLAC1 can be also activated by calcium-dependent protein kinases (CPKs; Geiger et al., 2010, Brandt et al., 2012). The majority of core ABA signalling

mutants express a strong ABA-insensitive phenotype (Koornneef et al., 1984; Merlot et al., 2002; Park et al., 2002; Hua et al., 2012)

1.2.4. High CO_2-induced stomatal closure

Plants have to sense CO_2 to provide sufficient carbon for photosynthesis and to control water use efficiency. Thus, CO_2 concentrations below ambient levels (~400 ppm) favour stomata to open while its elevated levels promote stomatal closure.

Overall, CO_2 passes into plant cells by diffusion through PIP2;1 aquaporin (A. THALIANA PLASMEMBRANE INTRINSIC PROTEIN 2;1) (Wang et al., 2016). βCA1 and βCA4 (BETA CARBONIC ANHYDRASES 1; 4) convert CO_2 to bicarbonate (Hu et al., 2010; Xue et al., 2011). As downstream mediators and SLAC1 are likely to be bicarbonate (HCO_3^-)-responsive proteins, this conversion is required for further signal transduction (Zhang et al., 2018b). It indicates that HCO_3^- rather than CO_2 acts as a signalling molecule in CO_2 signalling, although there is no genetic evidence for a CO_2/bicarbonate sensor so far (Tõldsepp et al., 2018).

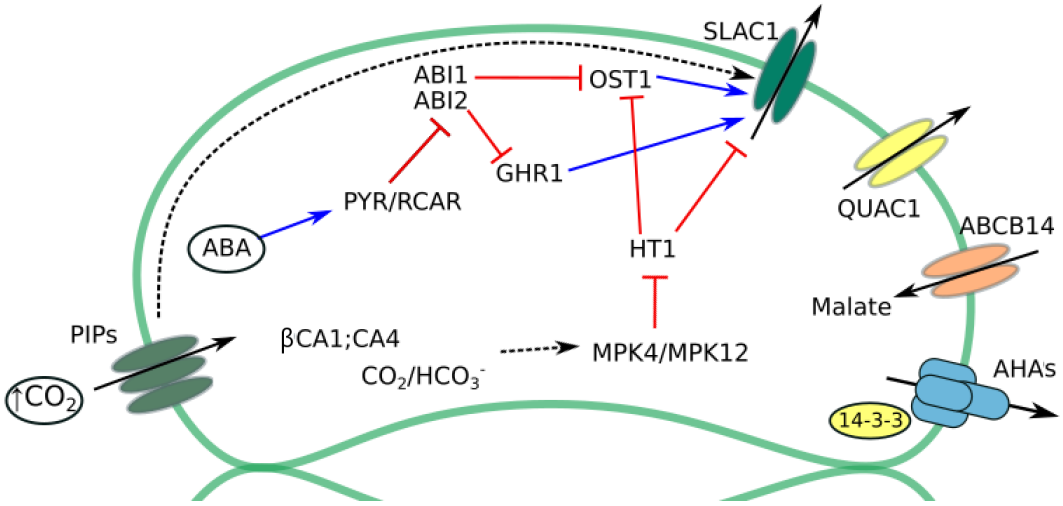

Figure 3. A scheme showing signalling pathways in ABA- and CO_2-mediated stomatal closure.
Solid lines represent confirmed interactions between signalling components: blue colour indicates activation and red colour shows suppression. Dashed lines display possible interactions. Under stress conditions, endogenous ABA is produced and bound by the PYR/PYL/RCAR receptor that forms a complex with ABI1 or ABI2. This releases OST1 and GHR1, respectively, which in normal conditions would be under ABI1/2 suppression. SLAC1 plays a central role in stomatal closure and is positively regulated by activated OST1 and GHR1. CO_2 enters cells through PIPs and is further converted to HCO_3^- with the help of βCAs. Elevated HCO_3^- concentrations mediate further signal transduction and activate MPKs kinases, which inhibit the activity of the HT1. CO_2 and ABA signalling pathways are known to converge at the level of OST1. Both HT1 and OST1 regulate the activity of SLAC1. QUAC1 anion channel, ABCB14 malate transporter and inhibition of AHAs have been shown to also contribute to CO_2 and ABA-related stomatal closure. (Details from Zhang et al., 2018a)

Downstream of these events, a regulator HT1 (HIGH LEAF TEMPERATURE 1) has been identified (Hashimoto et al., 2006). This entirely distinctive element in plant CO_2 sensing was

discovered in 2006 (Hashimoto et al.), when *ht1* mutants with disrupted CO_2 response were isolated. The HT1 protein kinase functions as a suppressor for SLAC1 activation by OST1 and GHR1 (Hõrak et al., 2016). HT1 itself is in turn under direct negative control by MPK4 and MPK12 (MITOGEN-ACTIVATED PROTEIN KINASES 4; 12) (Hõrak et al., 2016; Jakobson et al., 2016; Tõldsepp et al., 2018), which presumably are activated by increased HCO_3^- concentrations in guard cells. The *ht1* and *mpk12mpk4GC*, a mutant line where MPK4 has been specifically silenced only in guard cells, are the only lines showing completely impaired stomatal response to changes in CO_2 and unaffected response to ABA in intact plants (Hashimoto-Sugimoto et al., 2016; Tõldsepp et al., 2018).

Raschke (1975) found that ABA enhanced CO_2-induced stomatal closure, suggesting that pathways activated by these stimuli share some common components. Webb and Hetherington (1997) discovered a molecular interconnection between ABA and CO_2 signalling as plants carrying mutations in ABI1 or ABI2 displayed impaired response to both stimuli. More recently, other overlapping components in CO_2 and ABA signalling besides PP2Cs were identified, namely OST1, PYR/PYL/RCAR receptors, and CPKs (Merilo et al., 2013; Chater et al., 2015). SLAC1, the endpoint of signal transduction pathways in stomata, is also necessary for both responses (Negi et al., 2008; Vahisalu et al., 2008). Despite the close connection between CO2 and ABA signalling in guard cells, these two stimuli seem to activate SLAC1 through phosphorylation at different phosphorylation sites (Yamamoto et al., 2016), suggesting ABA-independent components in CO2 signalling. Despite of the received data, it has still remained unclear where exactly the signalling pathways downstream of ABA and CO_2 converge (Hsu et al., 2018) (Fig. 3).

1.3. *Arabidopsis thaliana* plasma membrane H^+-ATPases in stomata

The plasma membrane acts as a barrier between the cellular contents and the extracellular environment. The properties of plasma membranes are attributed to integral transport proteins. These transporters regulate movement of various substances in and out of the cells and participate in perceiving signals from the surrounding to initiate the cellular response towards environmental changes. Such plasma membrane-associated proteins are classified as pumps, carriers, and channels based on the differences in the forms of energy input and a speed of transporting molecules (Sussmann and Harper, 1989).

Proton pumps are among the most abundant proteins in plant membranes (Palmgren, 2001). There are two principal classes of proton pumps in plants: plasma membrane (P)-type and vacuolar (V)-type (Gaxiola et al., 2007). These transporters are a part of an active transport system and they require ATP as a source of energy. *Arabidopsis thaliana* plasma membrane H^+-ATPases are categorized as P3A-type pumps, as they are phosphorylated during the catalytic cycle and transport only protons (Pedersen and Carafoli 1987). P-type H^+-ATPases can be detected throughout a plant, although the cell types specialized in the transport of different solutes across the plasma membrane show higher expression of H^+ pumps (Palmgren, 2001). Stomata can be referred to as one of these examples. As described previously (chapter 1.2.1.), plasma membrane proton pumps play a central role in the regulation of stomatal opening. Their role is to create proton and membrane potential gradients across the plasma membrane, providing a control of nutrient transport and maintaining cell turgor. They are also related to salinity tolerance, cell growth and cellular pH homeostasis (Morsomme and Boutry, 2000).

Arabidopsis H^+-ATPases (AHAs) are encoded by a gene family consisting of 12 members (Axelsen and Palmgren, 2001; Baxter et al., 2003). The two highly expressed isoforms in plant tissues are closely related AHA1 and AHA2 (ARABIDOPSIS THALIANA H^+-ATPASE ISOFORM1; 2). The amino acid identity of these two proteins is 95% (Harper et al., 1990). Despite the fact that all of the AHAs are present in stomatal guard cells, AHA1, AHA2 and AHA5 are expressed in significantly higher levels than other members (Ueno et al., 2005).

1.4. The structure of major AHAs

The general structure and catalytic mechanism of all P-type ATPases appear to be conservative in the AHA family (Ekberg et al., 2010). Most information about AHAs is available due to studies of the model proton pump AHA2, after which other enzymes of the same type, including AHA1, have been characterized.

Both AHA1 and AHA2 are single polypeptides that are integrated into the plasma membrane (Sussmann 1994). Both proteins are similar in size: 948 and 949 amino acids, respectively (Harper et al., 1989; Harper et al., 1990). These proton pumps have five discrete domains: actuator (A), membrane (M), phosphorylation (P), nucleotide-binding (N), and regulatory (R) domains (Pedersen et al., 2007; Focht et al., 2017) (Fig. 4). The M-domain consists of ten transmembrane helices (M1-M10), with proton binding site(s) and a proton translocaton site

(Pedersen et al., 2007). The N-terminus of the pump is located at the A domain while 92 aa long C-terminus protrudes from a transmembrane M10 segment into the cytosol (Palmgren et al., 1991; Axelsen et al., 1999; Pedersen et al., 2007). This C-terminal extension is referred to as the R-domain due to its autoinhibitory function (described in chapter 1.6.) The cytoplasmic A-, N-, and P-domains assemble into a catalytic subunit that performs the ATP hydrolysis-mediated translocation of protons (Pedersen et al., 2007).

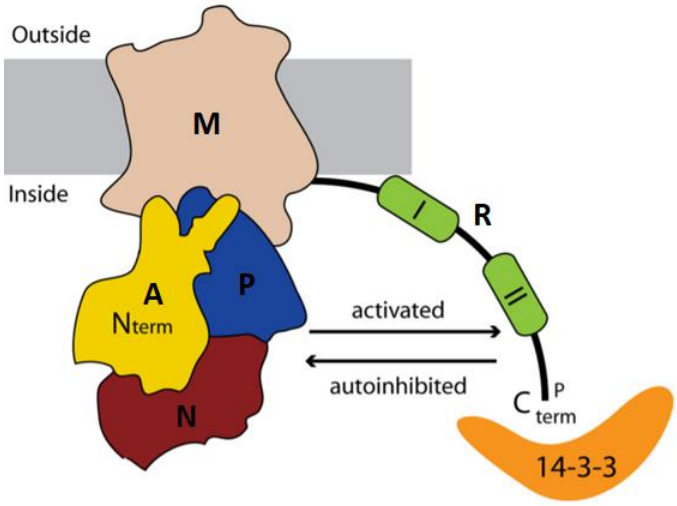

Figure 4. Schematic structural model of plant plasma membrane H^+-ATPase. Represented are five discrete domains of the P-type H^+-ATPase, specifically actuator (A), phosphorylation (P), nucleotide-binding (N), transmembrane (M) and regulatory (R) domains. Two autoinhibitory regions (I and II)-containing flexible C-terminal extension, also known as R-domain, encases the proton translocation site through interfering with cytoplasmic domains. The N-terminus was recently shown to assist R-domain in the enzyme autoinhibition. The proton pump will be activated when the penultimate residue is phosphorylated and/or the 14-3-3 protein is attached. (Ekberg et al., 2010 with modifications)

1.5. The catalytic cycle of H^+-ATPases

The catalytic cycle involves at least two conformational states of a proton pump, denoted as E1 and E2 (review in Jørgensen and Andersen, 1988). In the E1 conformation, the binding pocket is reachable for a proton from the cytoplasmic side. The conserved aspartyl residue (Asp-329 in AHA2 structure) in the P-domain is auto-phosphorylated by the N-domain coupled ATP (for further details see Pedersen et al., 2007; Jørgensen and Andersen, 1988). The phosphorylation transits the pump to the intermediate E1 state which possesses a strong affinity towards protons. The A-domain then dephosphorylates Asp-329 and the protein reaches the E2 configuration. In this state, the proton binding pocket is open to the apoplast and the pump acquires reduced affinity for protons. It leads to the release of the proton and the phosphate ion from ATP followed by the transition of the pump to the initial E1 conformation. The M-domain also contributes to proton transfer. A conserved Asp

residue at position 684 in AHA2 in (M6) is the single liable proton acceptor-donor (Buch-Pedersen et al., 2003a). Another residue, Arg-655 in M5, seems to assist with modulating Asp-684 to proceed with releasing the proton (Buch-Pedersen and Palmgren, 2003b).

1.6. Regulation of plant H^+-ATPases

Studies demonstrated that the activity of plant plasma membrane H^+-ATPases is regulated through post-translational modifications. Phosphorylation at different sites in AHAs may have an inhibiting or activating effect on proton translocation (reviewed in Rudashevskaya et al., 2012). Proton pump inhibition is related to formed intramolecular interactions that keep plant plasma membrane H^+-ATPases at a low activity state (Palmgren and Christensen, 1993; Ekberg et al., 2010). 14-3-3 proteins act as positive regulators for plant plasma membrane H^+-ATPases by anchoring R-domain and blocking autoinhibition (Jahn et al., 1997; Svennelid et al., 1999). The activation of H^+-ATPases may also occur without the assistance of 14-3-3 proteins and be only phosphorylation-dependent.

Autoinhibition of AHAs involves both ends of polypeptide chains (Palmgren and Christensen, 1993; Ekberg et al., 2010). The R-domain presumably anchors the A-domain and wraps around the entire cytoplasmic part of the enzyme, interrupting the catalytic cycle (Pedersen et al., 2007). A specific site in A-domain for this interaction has not been determined yet. A short 10 amino acid long N-terminal sequence seems to coat the R-domain and prevents phosphorylation (Ekberg et al., 2010). AHAs with removed or mutagenized termini showed increased rates of the pump activity (Palmgren et al., 1991; Ekberg et al., 2010).

The R-domain has a fundamental importance to the activity regulation of a proton pump as multiple plant growth regulating stimuli supposedly target this domain (Palmgren, 1991). Two autoinhibitory regions have been discovered in the AHA C-terminal extension. Residues Lys-863 to Leu-885 constitute the region I and Ser-904 to Leu-919 region II in the AHA2 apparatus. Alterations in the named residues abolish the inhibitory impact of the R-domain and result in an enhanced activity of a pump (Axelsen et al., 1999). The activation of a pump brings shifts in the pH optimum toward more neutral values and an increase in the affinity for ATP (lower Km value) (Regenberg et al., 1995).

For proton pump activation, the attachment of the soluble 14-3-3 proteins to the R-domain is important, whereas, phosphorylation of the penultimate Thr residue (Thr-947 in AHA2 or

Thr-948 in AHA1) creates a binding motif for 14-3-3 proteins (Jahn et al., 1997; Svennelid et al., 1999). Attached regulatory proteins are expected to relocate the autoinhibitory domain from the binding site in the cytoplasmic part of the enzyme (Pedersen et al., 2007). This clears the proton translocation site and reactivates proton pumping. The spatial organization of changes during the regulation of proton pump is not fully understood. A 14-3-3 protein dimer has been shown to bind with two proton pumps at once. However, suggested activated complex supposedly is a dodecamer and consists of six H+ -ATPase and six 14-3-3 molecules, forming a wheel-like structure (Kanczewska et al., 2005; Ottman et al., 2007).

Additional regulatory phosphorylation sites were mainly identified in the C- and N-terminal ends (Fig. 5). Phosphorylation of AHA2 Thr-881 also participates in pump activation (Fuglsang et al., 2014). On the contrary, sites Ser-931, Thr-924, Thr-551 and Ser-889 are in charge of pump inactivation and (might) prevent 14-3-3 proteins from binding (Rudashevskaya et al., 2012). Thr-551 is the only highly conserved phospho-residue found in P-domain, situated close to proton acceptor Asp-684. Discovered residues may also have a phosphorylating effect on adjacent sites (Duby and Boutry, 2009). Among all of the Ser/Thr protein kinases needed for the activity regulation of a proton pump, merely a few have been found (reviewed in Falhof et al., 2016). Another unresolved question is how the initial phosphorylation events are triggered.

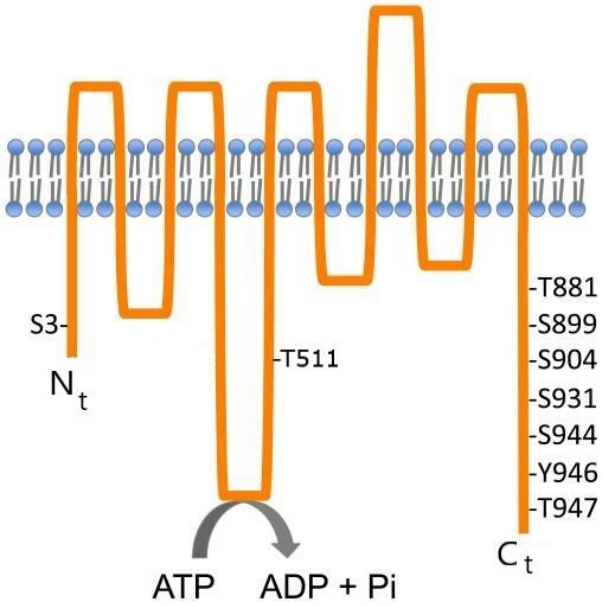

Figure 5. Identified phosphorylation sites in the amino acid sequence of AHA2 H^+-ATPase. Post-translational phosphorylation of Ser/Thr residues tunes the activity of the proton pump. Most of the phosphorylated residues are located in the termini of the protein. The cytoplasmic big loop that is responsible for ATP hydrolysis energizing proton translocation is shown in the scheme. (Haruta et al., 2015, altered)

1.7. Stomatal phenotypes related to AHA1 activity

AHA2 is considered by many researchers as a model pump for the AHA family and has been thoroughly studied, while AHA1 was demonstrated to play a most important role in stomata (Merlot et al., 2007). The double mutant lacking both AHA1 and AHA2 is embryo lethal. However, the single loss-of-function mutants have normal phenotypes under optimal growth conditions, suggesting the ability of the enzymes to at least partially compensate the lack of each other (Haruta et al., 2010).

The first genetic evidence indicating that dysregulated activity of proton pumps affects stomatal phenotypes was provided by identification of two dominant mutants with constantly active AHA1, rendering stomata open (Merlot et al., 2002; 2007). These mutants were named *open stomata 2-1D* and*2-2D* (*ost2-1D* and *ost2-2D*). The *ost2-1D* allele harbors the substitution of Pro-68 to Ser (P68S) and *ost2-2D* has two missense mutations L169F and G867S, with G867 actually causing the stomatal phenotype in the *ost2-2D* mutant as shown by the yeast complementation assays (Merlot et al., 2007). These amino acid substitutions in AHA1 lead to a decreased leaf temperature and enhanced water loss compared with wild-type plants due to constantly open stomata (Nuhkat, 2013). The *ost2-1D* mutant was derived from the wild-type Landsberg *erecta* accession and has necrotic lesions along with stunted growth (Merlot et al., 2002). At the same time, the growth phenotype of the *ost2-2D* mutant in the Col-0 background probably depends on growth conditions. Merlot et al. (2007) observed necrotic lesions in *ost2-2D*, but in the experiments carried out by Nuhkat (2013), the only noticeable discrepancy between the mutant plants and the wild-type was the shape of the leaves.

Both mutants were initially reported to be strongly ABA-insensitive in experiments on epidermal peels (Merlot et al., 2007). However, in experiments employing whole intact plants, both mutants demonstrate the responsiveness of their stomata to ABA (Nuhkat et al., 2013; Pantin et al., 2013). Furthermore, the gas exchange experiments conducted with intact plants demonstrated impaired responses to O_3 pulse, darkness and high CO_2 concentrations in *ost2* plants (Nuhkat, 2013).

2. EXPERIMENTAL WORK

2.1. Aims and objectives

Extensive research has provided in-depth knowledge about the model proton pump AHA2. AHA1 is considered to have matching attributes with AHA2 in general, but has not been studied so extensively. Recently, novel AHA1 mutants with constantly open stomata and potentially impaired stomatal response to high CO_2 have been discovered in a large-scale mutant screen for ozone sensitivity carried out jointly by Plant Signal Research Group in Tartu and Prof. Kangasjärvi's lab in Helsinki. The main aim of this thesis is to characterize the novel AHA1 mutants.

The following specific aims were followed:

1. To initiate backcrossing for the novel AHA1 mutants and to characterize the inheritance of their stomatal phenotypes;
2. To generate AHA1 transgenic lines expressing mutated versions of AHA1 and to examine their stomatal phenotypes.

2.2. Materials and methods

2.2.1. Identification of novel AHA1 mutants in a mutant screen

To get new knowledge about mechanisms of stomatal regulation, a large-scale screen was initiated to identify new components in guard cell signalling. Ozone sensitivity approach was used to recognise individual plants with defective stomatal closure. More open stomata in stomatal mutants enable an increased uptake of O_3 that is degraded to reactive oxygen species (ROS) in the apoplast and causes plant cell death. As a parental line, an *Arabidopsis* line expressing YELLOW CAMELEON 3.6 (YC3.6), a Ca^{2+}-sensitive fluorescent biosensor, in the Col-0 genetic background (Yang et al., 2008) was used. In 2012, approximately 125 000 seeds of YC3.6 were treated with ethyl methanesulfonate (EMS) to induce multiple point mutations and small deletions. Approximately 76 000 M1 plants were grown for seeds. About 380 000 M2 plants at the age of 2 weeks were exposed to O_3 (~350 ppb during 6 h). Plants with clear O_3-caused lesions were transferred to individual pots and studied with thermal imaging and water loss assay (Fig. 6). Later, the same approach was used for M3 plants to confirm phenotype stability. From 2014 to 2017, a pool of 551 lines was then analysed in Plant Signal Research Group in Tartu by using a gas exchange system designed for intact whole plants (Kollist et al., 2007; see also chapter 2.2.8.) to study stomatal closure in response to elevated CO_2, O_3, low humidity, ABA. Individual plants exhibiting impaired stomatal response to at least one applied stimulus were genotyped to reveal mutations in well-known stomatal regulators. Mutants without mutations in the studied genes are mapped to identify novel stomatal regulators. Among genotyped lines, novel AHA1 mutants were identified, which are characterized in this study. Backcrosses with some of the AHA1 mutants were started before the start of master studies.

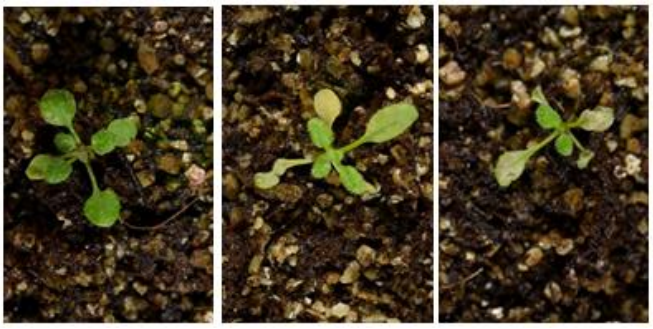

Figure 6. Scoring of *Arabidopsis* seedlings after exposure to O_3. Seedlings showing clear lesions (pictures in the middle and the right) were considered to have possible mutant phenotypes as the wild-type plants were unaffected by O_3 (in the left) (the courtesy of T. Vahisalu).

2.2.2. Used plant lines and bacterial strains

This study used *Arabidopsis* lines in the natural accession Col-0 genetic background. The pGC1::YC3.60 line (Yang et al., 2008) was used as a parental line in the large-scale screen and, thus, this line was employed as a control for the EMS mutants. The pGC1::YC3.60 transgenic line is further designated under the simplified name YC3.6 or YC in the backcrosses. The *aha1-6* line containing a T-DNA insertion in the *AHA1* promoter (Haruta et al., 2010) was used as the genetic background for transgenic lines described in this study. The *ost2-2D* mutant was described before (Merlot et al., 2007). The *slac1-4* and *ghr1-3* T-DNA mutants were characterized by Vahisalu et al. (2008) and Sierla et al. (2018), respectively.

Cloning procedures were performed in *Escherichia coli DH5α.* Genetic transformation of *Arabidopsis* plants was carried out with *Agrobacterium tumefaciens* GV3101.

All *Arabidopsis* mutants and bacterial strains are stored in the collection of Plant Signal Research Group.

Table 1. *Arabidopsis* lines used in the study

Line	Description	Background	Locus[1]	Alteration	Reference
Col-0	wilt-type				
ost2-2D	constitutively active H^+-ATPase	Col-0	AT2G18960	$AHA1^{G867S}$	Merlot et al., 2007
slac1-4	disrupted SLAC1	Col-0	AT1G12480	T-DNA insertion	SALK_137265; Negi et al., 2008; Vahisalu et al., 2008
ghr1-3	disrupted GHR1	Col-0	AT4G20940	T-DNA insertion	Sierla et al., 2018
aha1-6	knockdown AHA1 mutant	Col-0	AT2G18960	T-DNA insertion	SALK_016325; Alonso et al., 2003; Haruta et al., 2010
YC3.6	transgenic line	Col-0	-	YC3.6 Ca^{2+} sensor	Yang et al., 2008
G13/32B	EMS mutant	YC3.6	AT2G18960	$AHA1^{D165N}$	Waszczak et al., unpublished
T6-33	EMS mutant	YC3.6	AT2G18960; AT4G26080	$AHA1^{L432F}$; $ABI1^{I105V}$	Waszczak et al., unpublished
G19/34A	EMS mutant	YC3.6	AT2G18960	$AHA1^{A500T}$	Waszczak et al., unpublished

P34-32	EMS mutant	YC3.6	AT2G18960	AHA1^{M527I}	Waszczak et al., unpublished
G6/9D	EMS mutant	YC3.6	AT2G18960	AHA1^{G528E}	Waszczak et al., unpublished
T6-34	EMS mutant	YC3.6	AT2G18960	AHA1^{G528R}	Waszczak et al., unpublished
G5/47A	EMS mutant	YC3.6	AT2G18960; AT1G12480	AHA1^{E622K}; SLAC1^{G313E}	Waszczak et al., unpublished
aha1-6/AHA1^{M527I}	transgenic line	*aha1-6*	-	T-DNA insertion	this study
aha1-6/AHA1^{G528E}	transgenic line	*aha1-6*	-	T-DNA insertion	this study
aha1-6/AHA1^{G528R}	transgenic line	*aha1-6*	-	T-DNA insertion	this study
aha1-6/AHA1^{WT}	transgenic line	*aha1-6*	-	T-DNA insertion	this study
aha1-6/pH-GFP	transgenic line	*aha1-6*	-	T-DNA insertion	this study
Col-0/pH-GFP	transgenic line	Col-0	-	T-DNA insertion	this study
ost2-2D/pH-GFP	transgenic line	*ost2-2D*	-	T-DNA insertion	this study

1 According to the current Araport11 genomic annotation

2.2.3. Plant growth conditions

Before sowing, *Arabidopsis* seeds were stratified at least 3 days in distilled water at 4°C in order to stimulate germination. The seeds were sown on a soil mixture containing vermiculate (Vermipu), peat (Kekkilä), and tap water in the respective ratio of 4:2:3. Vermiculite in the mixture provides moisture control and prevents soil compacting. A transparent plastic overlay or Petri dishes were placed above seeds to retain moisture until shoots were visible.

Plants used for gas exchange measurements were grown in special rectangular plastic pots covered by fixed glass plates (as described in Kollist et al., 2007). The glass plate separates a plant rosette from the soil and prevents water vapour from soil to interfere gas exchange measurements. In the centre of the glass plates, there are tapered holes through which plants grow. Each pot contains 250 g of the soil mixture. The cavities around the plant stems were filled with a grafting wax 2-4 days before the experiments to prevent evaporation from the soil. Medium-sized pots (8.5x8.5x6.5 cm) were used to grow plants for water loss experiments and backcrossing. 2 or 4 plants were grown in pots filled with ~170 g of soil.

Extra seedlings from pots were removed after a week to leave only 1 plant to grow per at a spot. Seeds after agrobacterial transformation were also sown in medium-sized pots.

All the pots with seeds were incubated in growth rooms with light intensity of 90-150 µmol m^{-2} s^{-1}, day and night temperature at 22-24°C and 18-20°C, respectively, and the light/darkness periods of 12h/12h. After two weeks, plants for gas exchange experiments were transferred to growth chambers (Snijders Scientific, Microclima Arabidopsis, MCA16003lp6-E) and grown under the following conditions: 150 µmol m^{-2} s^{-1} light, 23°C / 18°C day/night temperature, 70% relative humidity and 12h photoperiod. Plants for water loss experiments were cultivated in the growth room under the same conditions. Plants for seed collection and backcrossing were grown in a long-day growth room (16h/8h photoperiod) to initiate flowering. Once the siliques turned brownish, watering was stopped and the plants were left to dry for at least 2 weeks before seed collection. All of the pots had drainage holes underneath and plants were bottom-watered every three days. Plants at the age of 3 to 5 weeks were used for water loss and gas exchange experiments.

2.2.4. Backcrossing of AHA1 mutants

Novel AHA1 mutants from the large-scale screen were backcrossed with the parental YC3.6 line to study stomatal phenotypes in F1 generation and to select back-crossed plants without unwanted mutations (Table 3). Since *G5/47A* also had a mutation in *SLAC1*, we also crossed this line with the *slac1-4* knockout mutant for the genetic complementation test. Plants were crossed by using the standard approach for *Arabidopsis*: unopen flowers were treated so only pistils were left, which were pollinated with pollen from another plant.

Table 2. List of the backcrosses performed in the study

Parental line 1	**Parental line 2**	**Resulting backcrosses**	**Related alteration(s)**
YC3.6	*G13/32B*	**YC x G13/32B**	AHA1 D165N
YC3.6	*T6-33*	**YC x T6-33**	AHA1 L432F; ABI1 I105V
YC3.6	*G19/34A*	**YC x G19/34A**	AHA1 A500T
YC3.6	*G5/47A*	**YC x G5/47A**	AHA1 E622K; SLAC1 G313E
slac1-4	*G5/47A*	**slac1-4 x G5/47A**	AHA1 E622K; SLAC1 G313E; T-DNA insertion in slac1-4
YC3.6	*slac1-4*	**YC x slac1-4**	DNA insertion in slac1-4

The plants resulted from backcrosses were verified by using cleaved amplified polymorphic sequence (CAPS) markers (Konieczny and Ausubel, 1993) or sequencing. Total genomic DNA from plants was isolated according to the Quick miniprep for plant DNA isolation protocol (Weigel and Glazebrook, 2009). CAPS assays included amplification of a locus-specific DNA fragment that was subsequently digested with an appropriate restriction endonuclease. DNA fragments were further loaded into 2-3% agarose gels containing ethidium bromide (0.5 µg ml^{-1}) and separated at a low voltage (50 V). CAPS markers were designed so that the cleavage pattern would differentiate mutated and wild-type alleles of AHA1. The markers were designed by using web-based program BlastDigester (http://bar.utoronto.ca/ntools-/cgi-bin/ntools_blast_digester.cgi) (BAR; version 1.4) and informatics platform Benchling (http://benchling.com/) (Table 4). If it was not possible to design a required CAPS marker, the genotypes were verified by sequencing to find successful crosses.

Table 3. CAPS markers developed and used in the study

				Expected fragment lengths (bp)	
Line	**Substitution in AHA1**	**Primers**	**Restriction enzyme**	**Mutant**	**WT**
G13/32B	D165N: Gat/Aat	ggaaaatggagtgaacaagagg tctctgtactttcggtgttgga	**LweI (SfaNI)**	445	173+272
T6-33	L432F: Ctt/Ttt	gactctgatggtaactggcaca aacacctagattcaacgcccta	**sequencing only**	-	-
G19/34A	A500T: Gcg/Acg	gtggtacccgagaaaacaaaag ttgtgctctgcaatcagtaacc	**TaiI (MaeI)**	109+116+273	225+273
G5/47A	E622K: Gaa/Aaa	atatgtatccatctgcggctct tagtgagaacggcactgatgat	**BspLI (NlaIV)**	29+378	29+340+38

2.2.5. Generation and verification of transgenic lines

Two plasmids, pART7 and pMLBart (Gleave, A., 1992), were used to construct plasmids for plant transformation (Fig. 7). *E.coli* carrying pART7 and pMLBart plasmids were selected on LB media plates (Duchefa Biochemie, 1.5% agar) supplemented with ampicillin (100 µg/ml) or spectinomycin (50 µg/ml), respectively. DNA ligase and restriction endonucleases were used according to manufacturer's recommendations (New England Biolabs and Thermo Fisher Scientific). Competent cells of E. coli DH5-*α* were prepared by the lab technician M. Välbe. An aliquot of competent cells was unfrozen on ice, mixed with a ligation mixture and incubated on ice for 10 minutes. Then, the cells were heat-shocked at 42°C for 90 s in a water bath, and placed back on ice for 2-3 min. 800 µl of LB medium were added to the cells which then were incubated at 37°C on a shaker (Labnet) for 30 min. The cells were collected

by brief centrifugation, resuspended in a small volume of LB medium and plated on a Petri dish with agarized selective media which then were incubated at 37°C overnight. Colonies were screened by using PCR to select correct genetic constructs. Then, 5 ml LB were inoculated with a selected colony and incubated with shaking at 37°C overnight. The obtained bacterial culture was used for plasmid isolation by using alkaline lysis protocol with Favorprep Gel/PCR purification mini kit (Favorgen).

High-fidelity Phusion DNA polymerase and the HF buffer (Thermo Fisher Scientific) were used for amplification of DNA fragments which were sequenced to avoid unwanted mutation after cloning. All of the primers were ordered from Mycrosynth AG (for the full list of the primers see Table 5). The 2.6 kb AHA1 promoter region was amplified using the primer pair AHA1prSacINotIF/AHA1pr-XhoI-Rw and cloned into the pART7 plasmid instead of the 35S promoter. Then, wild-type AHA1 was amplified from complementary DNA (cDNA) and cloned downstream to the native AHA1 promoter by using XhoI/BamHI restriction sites. Targeted mutations in the cloned AHA1 DNA sequence were introduced with QuickChange site-directed mutagenesis method (Liu and Naismith, 2008) to introduce M527I, G528E and G528R substitutions. The appropriate overlapping primers (Table 5) were designed with QuickChange Primer Design Program (Agilent) (https://www.agilent.com/store/primer-DesignProgram.jsp?toggle=uploadTrans&mutate=true&_requestid=95605) so that the targeted mutations were positioned near the centre of each primer. The PCR reaction for each construct of 50 µl contained ~2 ng of template DNA, 0.4 µM primer pair, 200 nM dNTPs and 1 unit of Phusion DNA polymerase. The PCR cycling parameters were 95°C for 30 s, 25 cycles of 95°C for 10 s, 70°C for 30 s and 2.5 min at 68°C with a final extension for 7 min at 72°C. The amplification reactions were treated with 1 µl of the DpnI restriction enzyme at 37°C for 1 hour to digest the template plasmid, followed by direct transformation into *E.coli* cells.

In order to facilitate measurements of proton concentrations in guard cells of transgenic lines, we introduced the pH sensitive green fluorescent protein pHluorins (Miesenböck et al., 1998; designated as pH-GFP in this work) under control of the SLAC1 promoter. The pH-GFP sequence was cloned under the SLAC1 promoter by D. Yarmolinsky previously. The expression cassette pSLAC1::pH-GFP was excised by using sequential digestion with SpeI (blunted with Phusion DNA polymerase) and NotI. The fragment was cloned into the binary pMLBart vector within the Ecl136II/NotI site. The resulted plasmid was named

pMLBart::pSLAC1::pH-GFP and was further used for cloning. The expression cassettes of pAHA1::AHA1 (wild-type or mutated) from pART7 were cut out as NotI fragments and were cloned into pMLBart::pSLAC1::pH-GFP.

The pMLBart-based constructs were then introduced into *A. tumefaciens* GV3101 strain by using chemical/heat shock transformation. The agrobacterium Ca^{2+}-treated competent cells were prepared by M. Välbe. 5 µl of a plasmid was mixed with 20 µl of competent cells, then the mixture was kept on ice for 10 min. Subsequently, heat shock treatment was performed at 37°C for 3 minutes and then the tubes were transferred back to ice for a short time. 600 µl of LB medium (Sigma-Aldrich) was added to the cells and incubated at 28°C on a shaker (Labnet) for 2 hours. Colonies containing the plasmids were selected on LB plates with 1.5% agar, 50 µg/ml spectinomycin and 25 µg/ml gentamycin.

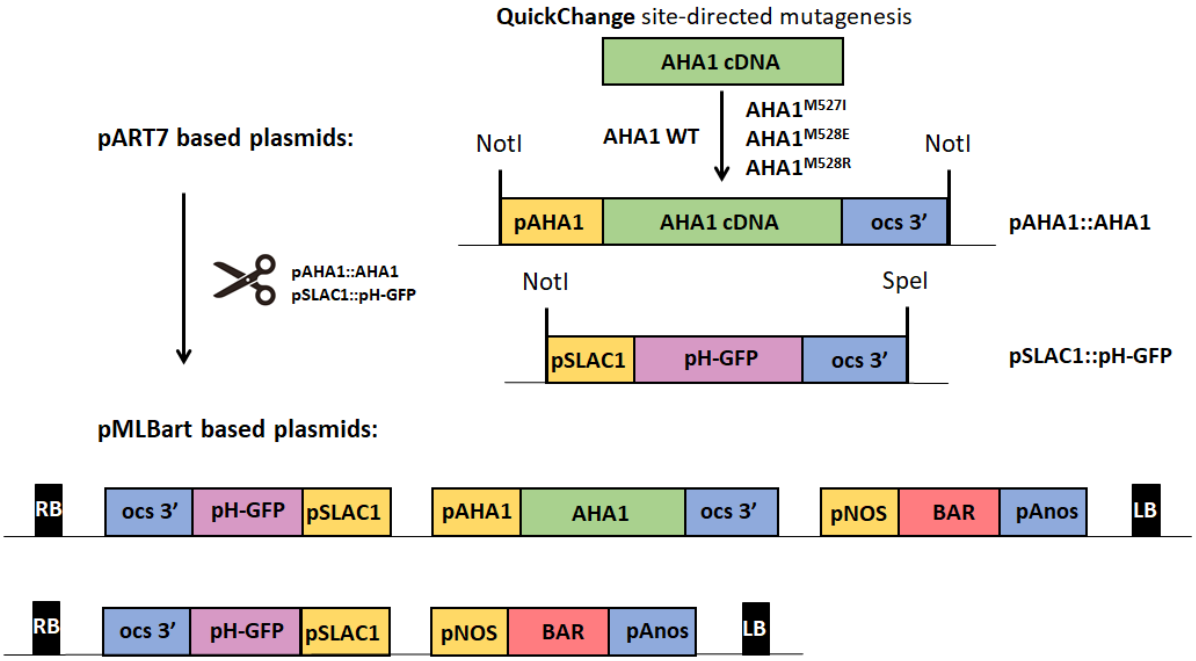

Figure 7. The scheme of generating constructs for plant transformation. $AHA1^{WT}$ sequence was amplified by using cDNA and then cloned into pART7 plasmid under the native AHA1 promoter. Targeted point mutations M527I, M528E and M528R were introduced into the cloned AHA1 sequence by using QuickChange site-directed mutagenesis. Before, pH-GFP was cloned into the pART7 plasmid under the guard cell-active SLAC1 promoter. The expression cassette pSLAC1::pH-GFP was cloned into the T-DNA region of the pMLBart vector, where the *BAR* gene is located. This plasmid was also used as a control vector and named pMLBart::pSLAC1::pH-GFP. The pAHA1:AHA1 cassettes with wild-type and mutated variants of AHA1 were inserted into pMLBart::pSLAC1::pH-GFP. As gene transcription terminators, octopine synthase (ocs 3') and nopaline synthase (pAnos) were used in the constructs. The sizes of the blocks in the picture are illustrative.

Arabidopsis plants were transformed by using the floral dip method (Clough and Bent 1998). Plants were grown in the long-day growth-room to induce fast flowering. First 3-5 cm long flower bolts were cut out to induce formation of a larger number of bolts. In 10 days, plants

continued flowering, and all formed siliques were removed to reduce number of untransformed seeds. To make starters, single colonies of the *Agrobacterium* strains for transformation were inoculated into 5 ml LB medium containing 50 µmg/ml spectinomycin and 15 µmg/ml gentamycin with following incubation during 48 hours at 28°C on a shaker. 2 ml of the culture was transferred into 200 ml LB medium with the same antibiotics, which then was incubated overnight under the same conditions. The agrobacterium cells were collected in 50 ml tubes by centrifugation at 4000 rpm (Eppendorf Centrifuge 5810 R) for 10 minutes. Then the supernatant was removed and the bacteria were resuspended in 50 ml of 5% sugar solution with 0.05% Silwet L-77 (Momentive). Arabidopsis bolts with unopen flowers were immersed into the agrobacterial suspension for 10-30 s. The pots with the plants were placed sideways into covered trays, containing wet wipes to retain moisture. The covers were removed in 24 h and the plants were returned to the long-day growth-room to produce seeds.

The *aha1-6* mutant with the T-DNA insertion in the promoter region in AHA1 gene was used as a background for the transgenic lines expressing the mutated AHA1 forms. Additionally, the *ost2-2D*, Col-0 and *aha1-6* lines were transformed with the plasmid containing only pH-GFP under the SLAC1 promoter. For simplification, the lines carrying the control vector are referred to as Col-0/pH-GFP, *aha1-6*/pH-GFP and *ost2-2D*/pH-GFP in the text. The pMLBart contains the herbicide glufosinate resistance gene *BAR* encoding phosphinothricin acetyltransferase under the nopaline synthase (nos) promoter. Resistance to glufosinate was used as a selection marker for transgenic lines. Collected T0 seeds from the dipped plants were germinated on soil and one week-old seedlings were daily sprayed 5 times with commercial Basta solution containing glufosinate (Bayer CropScience AG). 1 ml of original Basta solution per 800 ml distilled water was used for sprays. The glufosinate-resistant T1 plants were studied under a confocal microscope for detection of pH-GFP fluorescence (see chapter 2.2.7.). The T2 progeny of transgenic plants showing strong pH-GFP signal were studied in water loss and gas exchange experiments (chapters 2.2.8. and 2.2.9.). Numbers of T-DNA insertions in plant genomes of independent transgenic lines were estimated by analysing plant segregation after Basta spraying. Lines showing the ratio of 3 Basta-resistant to 1 Basta-sensitive plants were used for studies as they contain only one T-DNA insertion.

Table 4. List of primers used for cloning and sequencing in this study.

Name	Sequences[1] (5'→3')	Target region
AHA1prSacINotIF	AAAGAGCTCGCGGCCGCTACTCGTTTTATTCATTGGTAAAATT	AHA1 promoter
AHA1pr-XhoI-Rw	AAAACTCGAGCTTCACCCAGAAGAAATCAACA	AHA1 promoter
OST2-XhoI-Fw	AAAACTCGAGATGTCAGGTCTCGAAGATATCAAGA	AHA1 coding region
AHA1-BamHI-Rw	AAAGGATCCCTACACAGTGTAGTGATGTCCTGCT	AHA1 coding region
AHA1qc-M527I-Fw	GGCTTGGAATaGGAACCAATATGTATCCATCTGCG	QuickChange mutagenesis
AHA1qc-M527I-Rw	TATTGGTTCCtATTCCAAGCCTGCGACCGGTTTC	QuickChange mutagenesis
AHA1qc-G528R-Fw	GCTTGGAATGaGAACCAATATGTATCCATCTGC	QuickChange mutagenesis
AHA1qc-G528R-Rw	TATTGGTTCtCATTCCAAGCCTGCGACCG	QuickChange mutagenesis
AHA1qc-G528E-Fw	CTTGGAATGGaAACCAATATGTATCCATCTGCG	QuickChange mutagenesis
AHA1qc-G528E-Rw	CATATTGGTTtCCATTCCAAGCCTGCGACCG	QuickChange mutagenesis
pH-GFP-Fw	AAAAGGATCCATGAGTAAAGGAGAAGAACT	pH-GFP coding region
pH-GFP-Rw	AAAATCTAGATTATTTGTATAGTTCATCCATGC	pH-GFP coding region
ost2seq2R	CTGGAAAACTTCCTCAATCGG	AHA1 region
ost2seq4F	CCAAGCACCCTGGTCAAG	AHA1 region
ost2seq5F	CTGCTTTGACTTACATCGACTC	AHA1 region
ost2seq6F	CCAGGTTATGCCTTGCTTTCAG	AHA1 region
ost2seq7F	CCTGATAGCTGGAAGCTCAAAG	AHA1 region
pART7-seq-Rw	AATATCATGCGATCATAGGCG	pART7 vector
pART7pr-seq-Fw	GACCATGATTACGAATTTGGCC	pART7 vector
prAHA1seq1-Fw	CCAGTTGAATTAAACCATCATC	AHA1 promoter region
prAHA1seq2-Fw	AATTTAGTGTACTCACCACC	AHA1 promoter region
prAHA1seq3-Fw	CATGTATGTATTTTAAATTTTG	AHA1 promoter region
prAHA1seq4-Fw	CTGAAATTTTAATTATAAAACC	AHA1 promoter region
prAHA1seq5Rw	GACTTTTTGATCGTGCTGGGTC	AHA1 promoter region
SLAC1pr-seq-pr-Fw	AACCTGATTCATAAACAAAC	SLAC1 promoter region
pMLBart-seq-R	ATACGACTCACTATAGGGCG	pMLBart vector

[1] Introduced point mutations are indicated in small letters

2.2.6. Water loss assay

Water loss experiments were performed with five-weeks-old plants. From each plant 1-2 middle-aged leaves was excised and weighed immediately. Leaves were left to air-dry abaxial side up and were weighed again after 2 hours. Water loss was expressed as the ratio or percentage of fresh weight loss from the initial fresh weight.

2.2.7. Confocal microscopy

Confocal laser scanning microscopy was used as a method to select transgenic lines. LSM 710 META Laser Scanning Microscope (Zeiss) together with ZEN software (Zeiss) was used for confocal image acquisition. Leaves of 2 weeks old seedlings were collected and used to detect fluorescence of pH-GFP. Abaxial side of leaves was sequentially illuminated with 405 nm UV and 488 nm argon lasers. The emission light was collected in the region of 510-540

nm using illumination with each of the lasers. Brightfield and chlorophyll fluorescence (fluorescence in 650-680 nm) were also collected. The suitable sublines for subsequent research were selected based on visual pH-GFP expression intensity to use it for estimation of AHA1 activity in the future.

2.2.8. Gas exchange experiments

Measurements of stomatal conductance were used to indirectly characterize stomatal functioning. Higher values of stomatal conductance indicate enhanced water loss through stomata from the same leaf area and during the same time (expressed as mmol H_2O m^{-2} s^{-1}). The whole-plant time-resolved gas exchange analyses were performed using a custom-made device with 8 separate cylindrical chambers made of stainless steel (diameter of 7.8 cm and height of 3.5 cm) (detailed in Kollist et al., 2007) (Fig. 8). The device is coupled with a Li-COR (Li 7000) gas analyser that sequentially measures entering and leaving air composition (water and CO_2) for each chamber. The measurement results are collected by a computer and displayed in real time by in-house computer software that also controls the work of the gas exchange device. The program records the gas exchange data in text files. The concentrations of water vapour and CO_2 were measured every 4 min. Data acquisition for each chamber took 1 min: 30 seconds for the reference air flow (the air entering the chamber) and 30 seconds for the air flow from the chamber.

The rectangular-shaped pots described in chapter 2.2.3 are inserted into the cuvettes from below so the glass plate forms the bottom part of the chambers. The pots are underpinned by springs, pressing the glass plate of the pots tightly against polished edges of the chamber. Plants were pre-incubated in the chambers during 1 h to stabilized their stomatal conductance under standard conditions: ambient CO_2 (~400 ppm), 150 µmol m^{-2} s^{-1} light, 60-70% relative humidity, 24°C temperature.

A rise of CO_2 concentration (from ~400 ppm to ~800 ppm) was applied to induce stomatal closure. Each experiment included 4 plants. After application of high CO_2, stomatal conductance was recorded during 40 min. Before the experiments, photographs of all plants were taken with a Sony RX-100 camera and were used to measure leaf area using Fiji software (v1.52p). Taking into a consideration the plant area, corrected values of stomatal conductance were calculated with a specially designed program (Kollist et al., 2007).

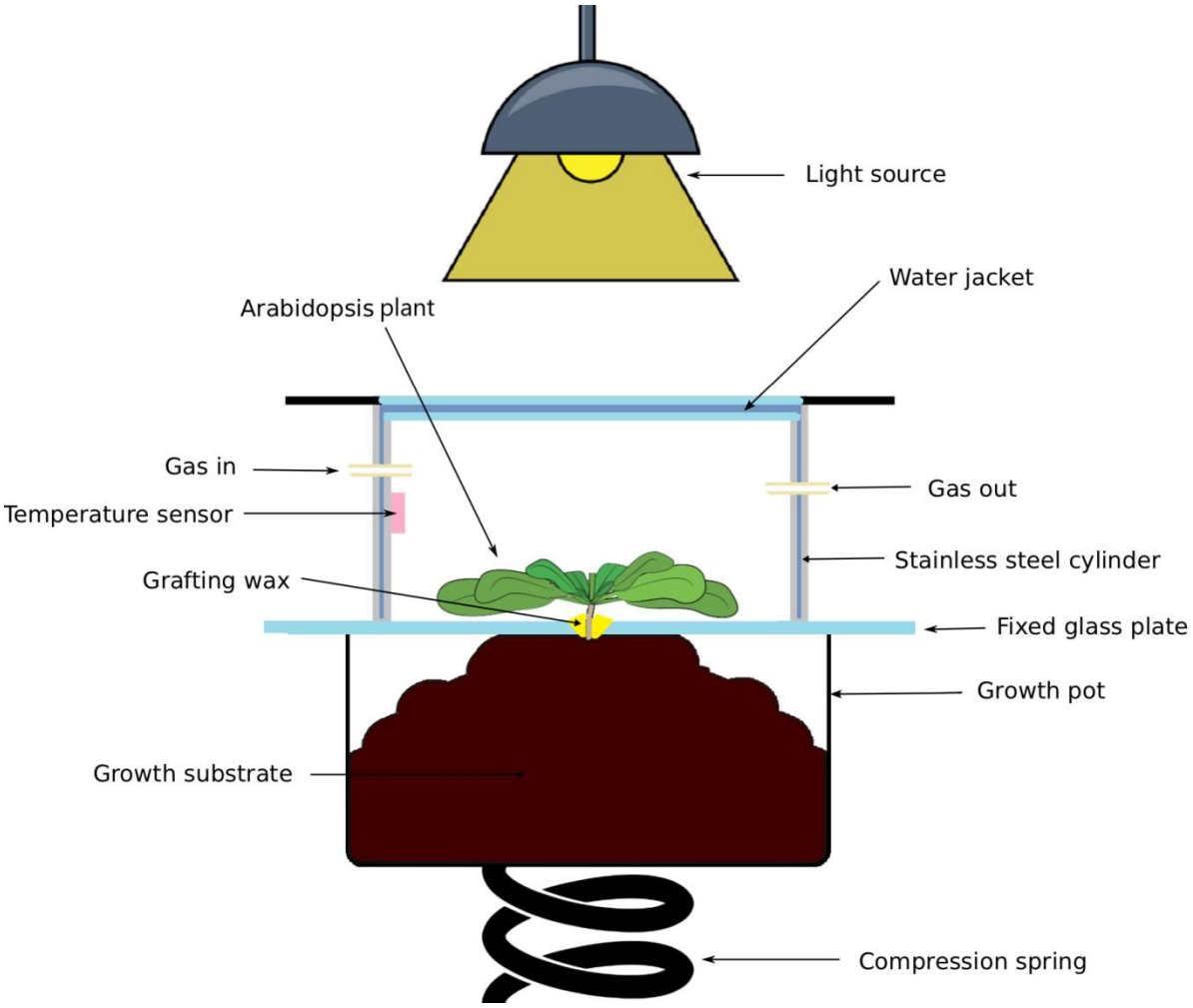

Figure 8. Illustration of the gas exchange measuring cuvette. Plants are grown in customized pots that can be attached to the measuring chambers with glass top. Pots are supported by springs. LED lights are placed above each chamber to provide suitable light for plant incubation. The surrounding water jacket in the measuring chamber keeps a uniform temperature during experiments. To monitor the internal temperature, a sensor has been attached to every chamber. The air entering and leaving the system is measured by a CO_2/H_2O analyser. The cavities around the plant stems should be filled with grafting wax.

2.2.9. Statistical analysis

Statistical data analysis was performed with JMP 8.0 software (SAS Institute Inc.). One-way analysis of variance (ANOVA) was used to compare the means of different groups and as a *post hoc* Tukey-Kramer HSD test was run. The significance level was set at $p<0.05$.

3. RESULTS AND DISCUSSION

3.1. The outcomes of the large-scale screen for stomatal regulators

The studies in this Master's thesis were conducted in the frames of the large-scale mutant screen which was aimed to discover novel stomatal regulators and novel alleles of proteins involved in stomatal signalling (Waszczak et al., unpublished). In this forward genetic screen, M_2 plants grown from EMS-treated YC3.6 seeds were exposed to O_3 to select individual mutants with clear O_3-induced damages. As supplementary methods, water loss assays and thermal imaging were used to identify mutants with impaired stomatal functioning among the O_3-sensitive plants. The progeny of the selected plants was studied in the secondary screen using the same methods to confirm the plant phenotypes. The gas exchange analysis (Kollist et al., 2007) in 551 most interesting lines demonstrated impaired stomatal responses to elevated CO_2, ABA spray, O_3 pulse, and a reduction of air humidity (elevated vapour pressure deficit) in 35%, 30%, 29% and 21% of the studied lines, respectively. In the genomes of the most promising mutant lines with impaired stomatal closure, 26 selected loci of well-characterized stomatal regulators were sequenced to avoid re-discoveries of these proteins (Fig. 9). This analyse detected 151 novel alleles affecting the coding regions of the stomatal regulators and 79 mutants without any mutations in the studied regions.

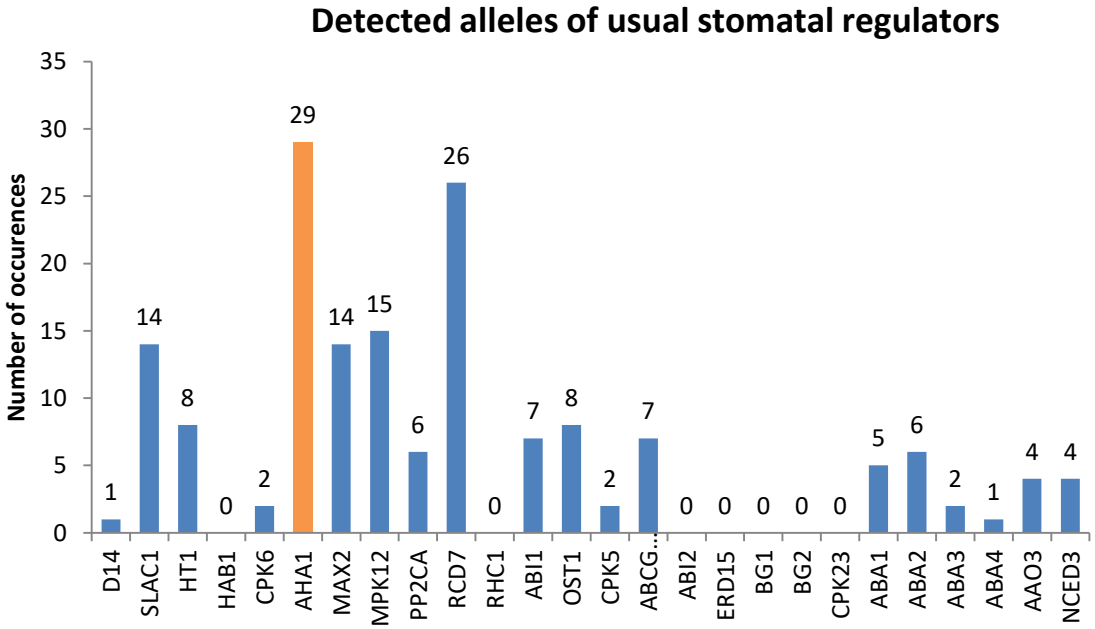

Figure 9. Identified mutations in the genomic regions of the mutants discovered in the large-scale screen carried out in Helsinki and Tartu. 26 encoding regions encoding stomatal regulators were sequenced to detect their alleles potentially causing mutant stomatal phenotypes. Genetic alterations in AHA1 were the most frequent (indicated with orange colour). In some genes, no mutations were identified.

Interestingly, the sequencing of the known stomatal regulator genes revealed 29 amino acid substitutions in the gene encoding the AHA1 proton pump (Fig. 9). This indicates that mutations in AHA1 were preferably selected during the screen for ozone-sensitive plants. Previously, stomatal phenotypes of the AHA1 mutants *ost2-1D* and *ost2-2D* with constitutively open stomata (Merlot et al., 2007) were studied in The Plant Signal Research Group (Nuhkat, 2013). The discovery of novel AHA1 alleles and our previous studies of the *ost2* mutants led us to characterize how newly-discovered mutations in AHA1 affect stomatal functioning. Previously, novel GHR1 alleles identified in the large-scale screen were employed to elaborate functions of GHR1 in stomatal regulation (Sierla et al, 2018). It shows that the forward genetic screen using ozone sensitivity approach provided not only stomatal mutants where novel components in guard cell signalling can be discovered, but also valuable genetic material for studies of stomatal regulators.

3.2. Newly-identified mutations in AHA1

The point mutations in the *AHA1* gene affected 14 different sites of the AHA1 polypeptide chain (Fig. 10). The amino acid changes most frequently affected G528 with two distinctive variants. One of those variants, Gly-528 to Arg was detected much more frequently than any other alterations in AHA1. Interestingly, we also found an amino acid substitution that affected M527 in the close vicinity to G528. It might indicate that this site is of significant importance for AHA1 functioning. Another abundant mutation in AHA1 was the previously discovered G867S substitution corresponding to the *ost2-2D* mutation (Merlot et al., 2007).

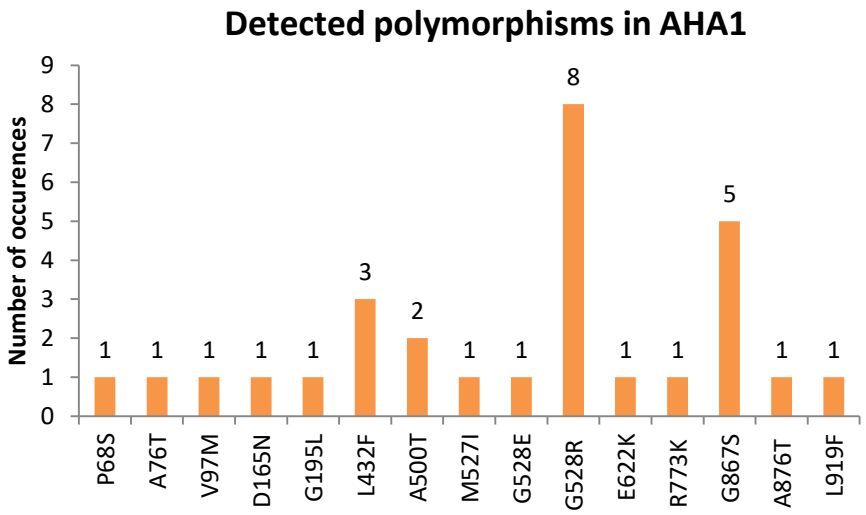

Figure 10. Point mutations in the AHA1 coding region identified during the mutant screen. A total of 29 amino acid substitutions in the gene encoding the AHA1 proton pump were revealed in 14 different sites.

The higher frequencies of mutations in G528 and G867 can indicate importance of these sites for AHA1 functioning. Among the identified mutations, the P68S amino acid substitution known as *ost2-1D* was observed in one line (Merlot et al., 2007). The amino acid residues which were affected by newly-identified mutations have not yet been previously shown to have any function in the regulation or the catalytic activities of AHA1 or AHA2 (Buch-Pedersen and Palmgren, 2003a,b; Pedersen et al., 2007; Rudashevskaya et al., 2012). The previously documented regulatory mutations in the plasma membrane proton pumps were mostly detected in the R-domain. The only exceptions are phosphorylated T511 and S3 in AHA2 and the AHA1 P68 in the *ost2-1D* mutant, affecting the phosphorylation (P) and actuator (A) domains (Merlot et al., 2007; Rudashevskaya et al., 2012). The mutations found in the large-scale screen are located not only in R-domain but also in the A- and P-domains (Fig. 11). It was ascertained that the detected mutations in AHA1 are predominantly located in the cytoplasmic regions of the protein, although two mutations are in the transmembrane domains.

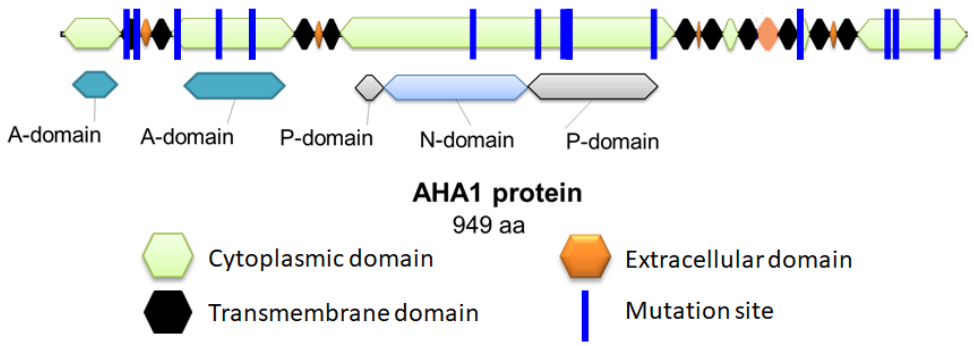

Figure 11. Positions of the newly-identified AHA1 mutations in the screen. The topology of AHA1 is depicted according to the Uniprot database (P20649). The domains responsible for the catalytic activity are shown as in the highly similar AHA2 protein (Pedersen et. al., 2007).

The phenotypic studies of *ost2-1D* and *ost2-2D* demonstrated that these mutants are prone to wither even in well-watered conditions (Merlot et al., 2007) due to enhanced stomatal apertures (Fig. 12) and excessive water transpiration from leaves. Constantly open stomata that are not able to close in response to O_3 in these *ost2* mutants (Nuhkat, 2013) made possible their selection in the screen based on O_3-sensitivity. The same reasons apparently determined selection of novel AHA1 mutants if these mutations in AHA1 similarly lead to constitutive activation of proton pump.

It should be noted that EMS mutagenesis produces multiple randomly distributed mutations into various locations of the plant genome. Indeed, in 3 AHA1 mutants, additional mutations were detected in other sequenced genes (Table 6). Furthermore, as possible mutations were

detected only in the selected loci, genetic alterations could also emerge in unexamined regions of the genome. Hence, it is not possible to rule out that the mutations in other unknown stomatal regulators caused observed stomatal phenotypes. It is of utter importance to determine which of the mutations in an EMS mutant was responsible for the observed stomatal phenotype. Possible solutions could include backcrosses with the parental line to eliminate unwanted mutations or generation of transgenic plants for expression of mutated forms of AHA1. In our further studies, we decided to backcross all the AHA1 mutants and to generate transgenic plants for expression of the most frequent mutant forms of AHA1 identified in the screen.

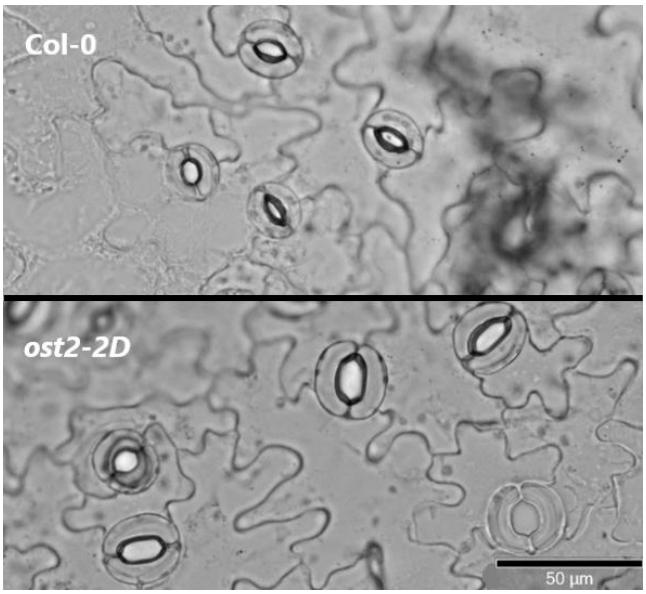

Figure 12. Brightfield pictures of epidermal peels with light pre-opened stomata of *ost2-2d* and Col-0 under a light microscope. The *ost2-2D* mutant has visually more open stomata in contrast to the wild-type Col-0. The picture was taken from the thesis author's previous experiments (Unt, 2018).

3.4. Characterization of AHA1 mutations by yeast complementation assays

Biochemical studies of AHAs were long time complicated for plant transformation due to the presence of various AHA isoforms sharing overlapping functions (Palmgren, 2001; Axelsen and Palmgren, 2001; Baxter et al., 2003; Haruta et al., 2010). Since then, the yeast complementation assay has been widely used as a tool to characterize regulation and activity of plant H^+-ATPases. For example, constitutive activity of AHA1 in the *ost2* mutants was confirmed by using yeast complementation analysis (Palmgren and Christensen, 1993; Merlot et al., 2007; Ekberg et al., 2010). In order to study activities of novel mutated AHA1 versions, we established collaboration with the Prof. Palmgren lab where this method is frequently used (Fig. 13).

All of the newly-identified AHA1 mutations were used in yeast complementation assays, excluding AHA1^{V97M}, AHA1^{G195L} and AHA1^{L919F} that were discovered later and will be used in the further experiments. The yeast complementation analysis is based on expression of plant H^+-ATPases in the yeast *Saccharomyces cerevisiae* strain RS-72, where native pump Pma1 (PLASMA MEMBRANE ATPASE 1) is expressed under a galactose-inducible promoter and turned completely off when galactose is not present (Cid et al., 1987; Villalba et al., 1992). Thus, complementation of Pma1 by plant H^+-ATPases can be studied on synthetic media not containing galactose. As reported before, plant H^+-ATPases exhibiting auto-inhibition are not able to support yeasts growth. Importantly, AHAs with truncated termini due to lacking of regulation could efficiently rescue yeast growth and allow cells to grow at low pH values in a medium (Palmgren and Christensen, 1993; Ekberg et al., 2010).

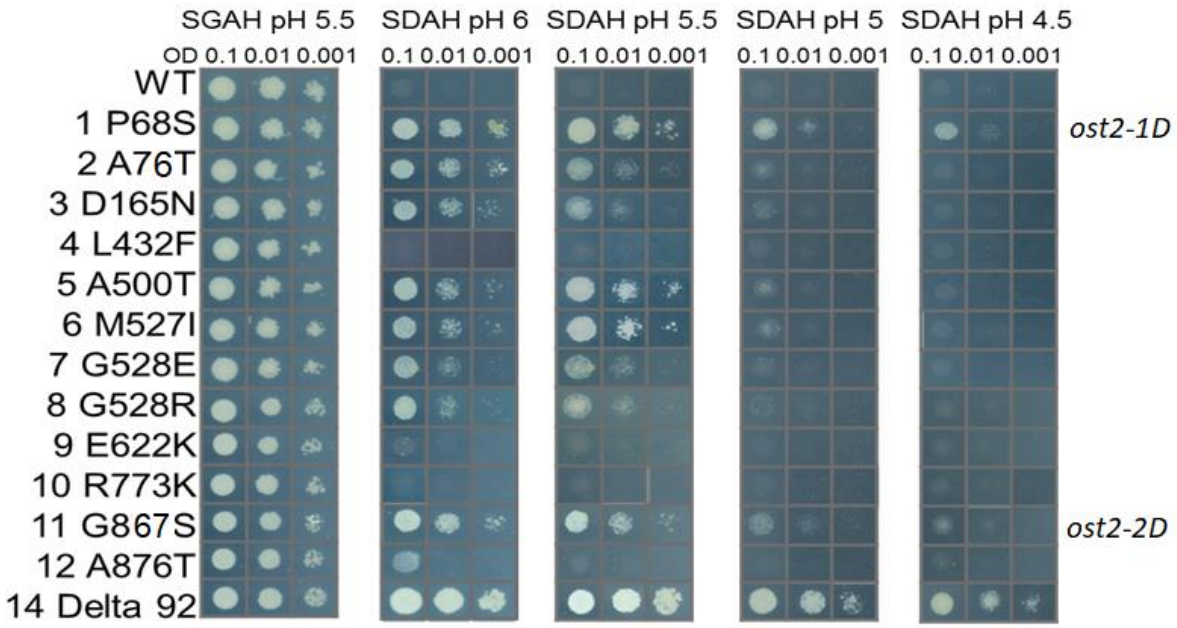

Figure 13. Yeast complementation analysis for new AHA1 alleles carried out in Prof. Palmgren's laboratory. The yeast strains containing wild-type (WT) and mutated AHA1 in dilutions of 0.1, 0.01, 0.001x were tested for growth at various pH values on a synthetic medium containing either galactose (SGAH) or glucose (SDAH). As expected, WT AHA1 in yeasts showed growth only when galactose was present and AHA1 with deleted R-domain (Delta 92) had growth even at low pH values without galactose. P68S and G867S mutations present in *ost2* mutants showed at least some growth at all pH values on glucose medium. Three of the analysed mutations, L432F, E622K, R773K, could not complement the absence of the native proton pump in yeasts. All other tested strains displayed abilities to complement yeast growth in the range between the WT AHA1 and AHA1 with *ost2* mutations.

In the experiments conducted by Prof. Palmgren lab, the RS-72 yeast strain expressing AHA1 with totally truncated C-terminus showed efficient growth even at pH 4.5. At the same time, the yeast cells with wild-type AHA1 were not able to grow without galactose in the pH range from 4.5 to 6.0. The AHA1 P68S and G867S mutation could also complement the yeast native

proton pump as shown Merlot et al. (2007). AHA1 variants with mutations discovered in the large-scale mutant screen did not allow yeasts to growth at lower values than pH 5.5. Nevertheless, most of the AHA1 strains still supported the growth of yeasts, meaning these mutations could be involved in regulating AHA1 activity state in plants. Those verisons not able to complement the yeast proton pump may represent silent mutations and the certain phenotype in those plants could be triggered by other mutations in *Arabidopsis* genome. However, plant proton pumps may operate differently in yeasts and no final conclusion can be drawn solely on the basis of yeast complementation assays.

3.5. Stomatal phenotypes related to newly-identified mutations in AHA1

Even though the properties of the plant plasma membrane H^+-ATPases were characterized by complementation assays in yeasts, these experiments cannot verify the functional role of the identified mutations in AHA1 *in planta*. The gain-of-function AHA1 mutations cause stomatal phenotypes (Merlot et al., 2007) which can be detected even when unaffected AHA1 is expressed. The earlier whole-plant gas exchange experiments with a limited number of plants demonstrated that the majority of AHA1 mutants exhibited fully or partially impaired response to high CO_2 (Table 5). The *ost2-1D* and *ost2-2D* lines isolated by Merlot et al. (2007) as well as in the large-scale mutant screen demonstrated the absence of stomatal closure in high CO_2 concentrations (Nuhkat, 2013). Interestingly, $AHA1^{A876T}$ mutant displayed wild-type stomatal CO_2 response. Most likely, this mutant was discovered due to its higher water loss, which also can result from mutations in AHA1 (Merlot et al., 2007). AHA1 with this mutation showed only a weak degree of complementation in the RS-72 yeast (Fig. 13), indicating that activation of AHA1 in this EMS mutant was not sufficient for the suppression of high CO_2-triggered stomatal closure.

One of the aims in this study was to initiate backcrosses with the EMS AHA1 mutants and to characterize stomatal phenotypes in the F1 generation. As already stated, EMS mutagenized plants often carry numerous mutations that may contribute to the development of an emerged phenotype. Backcrossing of an EMS mutant with its progenitor multiple times is used to determine a causal mutation(s) and remove all other mutations (Weigel and Glazebrook, 2008). During each backcross, half of the genome is replaced with the parental line genome. Then, within the progeny population, plants displaying a mutant phenotype are selected for further crosses, reducing unwanted genetic changes. In addition, the inheritance

type of a mutant phenotype can be examined in the progeny resulting from the crosses. In F1 heterozygous plants, a dominant allele affects plant functioning while phenotype caused by a recessive allele is not detected.

The mutants carrying newly-identified AHA1 mutations were crossed with the parental line YC3.6. The F1 progeny of these crosses was examined in gas-exchange experiments by using high CO_2 (~800 ppm) in a custom-made gas exchange device (Kollist et al., 2007). Due to a large number of mutants, this work was performed together with M. Nuhkat and D. Yarmolinsky (indicated in Table 6). The information about the backcrossed AHA1 mutant lines and the progress in their analysis are shown in Table 6. The correctness of the backcrosses was verified by using CAPS markers or sequencing (Fig. 14).

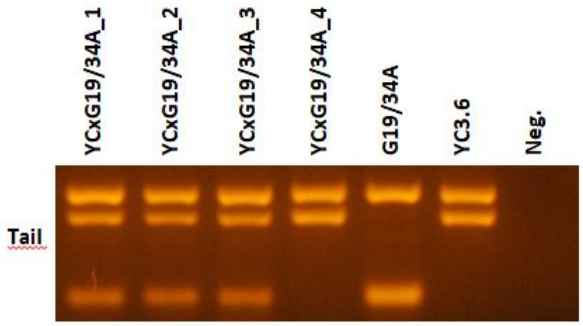

Figure 14. An example of CAPS marker bands generated by amplification of the corresponding genomic region in G19/34A EMS mutant line and its backcrosses with YC3.6, followed by digestion with the Tail restriction enzyme. The used primer pairs for PCR and expected fragment lengths after the cleavage are shown in Table 3. Neg. – negative control amplified without genomic DNA. The amplified PCR fragments corresponded to the expected sizes according to a DNA ladder (not shown). The forth from the left bands show that the plant resulted from self-pollination of YC3.6 and was excluded from the results.

The results showed that the majority of the substitutions of the selected AHA1 mutants behaved in a dominant or a semi-dominant fashion (Table 6). As examples, the gas exchange results obtained within the framework of this Master's thesis are presented (Figure 15). The *G13/32B* mutant (Fig. 15A) with $AHA1^{D165}$ had a steady-state stomatal conductance close to that of parental line YC3.6 as well as that of the backcrossed F1 plants. Both the *G13/32B* mutant and the F1 plants did not respond to the increase of CO_2. A complete impairment of the stomatal response to high CO_2 was also observed in the *T6-33* and YC x *T6-33* (Fig. 14B), although the steady-state stomatal conductance in the F1 plants was slightly decreased. The high CO_2 stomatal responses in F1 YC x *T6-33* and YC x *G13/32B* are similar to those in *T6-33* and *G13/32B* suggesting that D165N and L432F mutations in AHA1 are dominant. The application of high CO_2 induced 18% decrease in stomatal conductance of the F1 YC x *G19/34A* plants (Fig. 15C), although stomatal closure in these plants was approximately 2

fold less than in the YC3.6 plants. This suggests that the AHA1 A500T mutation in this line is semi-dominant, since the intermediate phenotype was detected in the heterozygous plants. In contrast to the other three described mutants, *G5/47A* exhibited a partial impairment of high CO_2 induced stomatal closure. Also, the F1 YC x *G5/47A* plants (Fig. 15D) clearly demonstrated a wild-type-like decrease in stomatal conductance in response to high CO_2. Previously, *G5/47A* showed enhanced stomatal conductance in experiments carried out by M. Nuhkat, although stomatal responsiveness was similar. The gas exchange experiments for this line should be repeated to clarify the stomatal phenotype.

In the future, desirable backcrossed plants showing dominant trait will be selected and the backcrossing procedure will be continued. The plants showing recessive traits cannot be directly selected from the F1 generation and for this reason, are allowed to self-pollinate before the selection process. Each subsequent backcross reduces the likelihood of secondary mutations in the mutant line. Therefore, in the next phases it is possible to genotype the plants to determine the causal mutation.

Table 6. General information about mutants carrying substitutions in AHA1 coding region.

Alteration in AHA1	Related line	Accompanying mutations	Response to ↑CO_2[1]	Backcrossed	Response to ↑CO_2[1] in F1
P68S	G22/28A		++	Yes	++
A76T	G9/19C	ABA4 R177W	+	Yes	-
V97M	E15-6		++	No	na
D165N	G13/32B		++	Yes*	++
G195L	M5		++	Yes	na
L432F	T6-33	ABI1 I105V	++	Yes*	++
A500T	G19/34A		++	Yes*	+
M527I	P34-32		++	Yes	+
G528E	G6/9D		++	Yes	+
G528R	T6-34		++	Yes	++
E622K	G5/47A	SLAC1 G313E	+	Yes*	-
R773K	G8/39D		+	Yes	-
G867S	T19-34		++	No	++
A876T	G6/22B		+	Yes	-
L919F	P2/2		+	Yes	+

1 "-" – wild-type response; "++" – strongly impaired response; "+" – somewhat impaired response; na – not analysed. * - backcrossed in this study

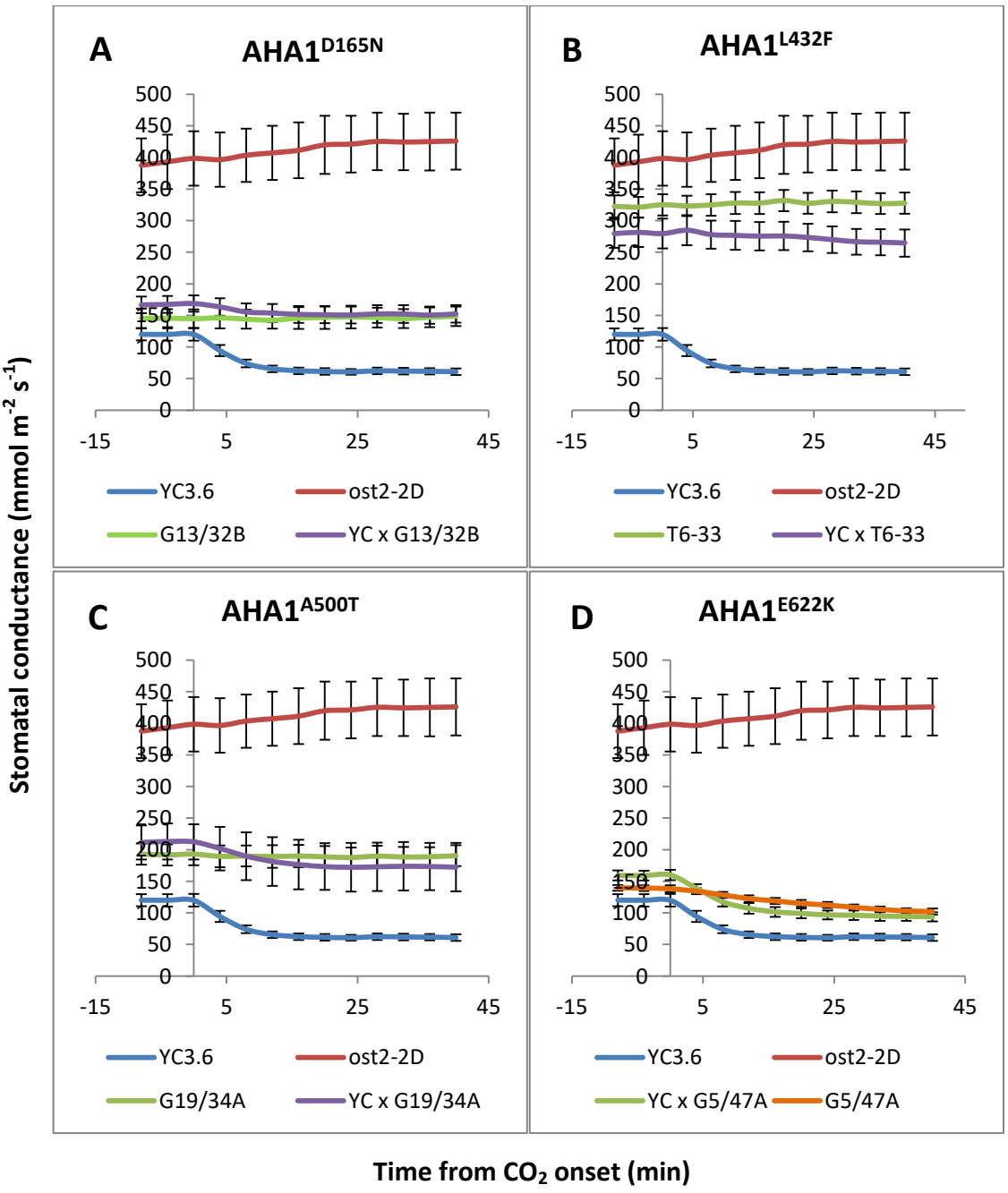

Figure 15. Elevated CO_2 responses in the newly-identified AHA1 mutants and in the plants resulted from their crosses with the YC3.6 line. 4 EMS mutants and their backcrosses with the parental line were studied in this Master's thesis. Graphs represent the time-resolved stomatal conductance measurements for (A) *G13/32B*, (B) *T6-33*, (C) *G19/34A,* and (D) *G5/47A* mutant lines. High CO_2 (elevation of CO_2 concentration from 400 to 800 ppm) was applied at time 0. The values are mean ±SEM (n=6-8).

3.6. Additional mutations in the AHA1 mutants

Besides mutations in the AHA1 coding region, 3 of 15 lines contain additional genetic alterations in other sequenced genes encoding stomatal regulators (Table 6). Thus, point mutations were detected in *SLAC1*, *ABI1* and *ABA4* (*ABSCISIC ACID DEFICIENT 4*) genes.

The *slac1* mutants lacking the main anion channel in guard cells have reduced responsiveness to almost all environmental signals regulating stomatal closure (Negi et al.,

2008; Vahisalu et al., 2008). Stomatal closure in response to O_3 and elevated CO_2 in *slac1* is severely impaired (Vahisalu et al., 2008), suggesting that the SLAC1^{G313E} substitution could be the phenotype-causing mutation in the *G5/47A*. Besides, *slac1* alleles in *Arabidopsis* are recessive (Vahisalu et al., 2008) and result in constitutively higher stomatal conductance than in wild-type plants only in homozygous plants (Negi et al., 2008; Vahisalu et al., 2008). These notions are consistent with the obtained gas exchange results for the *G5/47A* mutant (Figure 14). In order to confirm that the phenotype of *G5/47A* line could potentially be related to G313E substitution in SLAC1, a complementation test was performed. The *G5/47A* mutant was backcrossed with parental line YC3.6 as well as the *slac1-4* knockout mutant. To affirm the recessive inheritance of the *slac1-4*, this line was crossed also with the YC3.6. Plants resulted from the crosses were verified by using CAPS markers and only successfully crossed plants were involved in the results.

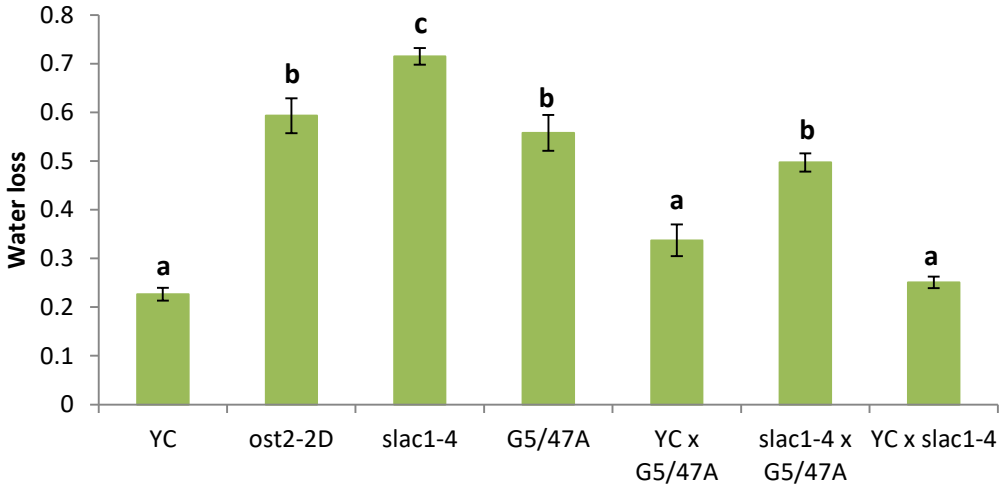

Figure 16. The complementation test with the newly-identified *G5/47A* AHA1 mutant that carries an additional point mutation in SLAC1. The *G5/47A* was crossed with the *slac1-4* knockout mutant and with YC3.6. Additionally, *slac1-4* was crossed with YC3.6. Complementation was studied in the F1 plants and the parental lines by water loss assay. Letters denote statistically significant differences between the phenotypes (one-way ANOVA with Tukey-Kramer HSD *post hoc* test, $p<0.05$) and the values are mean ±SEM ($n\geq5$-8).

As *slac1-4* has a very high water loss from detached leaves (Vahisalu et al., 2008), stomatal phenotypes in the *G5/47A*-related lines were studied by using water loss assays. The *ost2-2D* was added to the experiments as a known AHA1 mutant. It is apparent that *slac1-4* in the heterozygous state in the YC x *slac1-4* cross demonstrated the same water loss as that of YC3.6, confirming that it is clearly a recessive allele. At the same time, YC3.6 x *G5/47A* F1 plants did not statistically differ from YC3.6 and YC x *slac1-4* F1 plants, suggesting the

recessive inheritance of the causal mutation in the *G5/47A* as it was also shown by the gas exchange experiments (Figure 14). The water loss of *G5/47A* and *slac1-4 x G5/47A* was not significantly different from each other and was higher than in YC3.6. Hence, crossing *G5/47* with *slac1-4* did not influence *G5/47* mutant phenotype, meaning that G313E substitution in SLAC1, not AHA1^{E622K}, was responsible for the stomatal phenotype. The G313E mutation in SLAC1 seems to have less damaging effect on stomatal functioning than the complete knockout of the SLAC1.

The *G9/19C* line was additionally carrying a mutation in the site R177W of ABA4. ABA4 catalyses an intermediate step in ABA biosynthesis and, therefore, *aba4* mutants can have reduced ABA content and slightly enhanced stomatal conductance (North et al., 2007; Merilo et al., 2018). In addition, ABA4 regulates antioxidant properties of photosynthetic apparatus and ABA4 deficient plants could be more susceptible to O_3/ROS (Dall'Osto et al., 2007). The *aba4* mutants have not been previously tested to high CO_2 regulations. However, other ABA-deficient mutants respond normally to CO_2 elevation (Merilo et al., 2013, 2015; Hsu et al., 2018), which leads to an understanding that impaired CO_2 response in the *G9/19C* mutant is not caused by the mutation in ABA4. Besides, the AHA1^{A76T} substitution was clearly active in the yeast complementation assay (Fig. 13), which shows an association between the AHA1 mutation and the resulting phenotype. It is possible that mutation in ABA4 only enhanced stomatal conductance and facilitated the selection of the *G9/19C* mutant in the screen. In the future, it is important to eliminate this specific mutation by backcrosses to study the AHA1^{A76T} substitution.

A mutation in ABI1 accompanied the AHA1^{L432F} substitution in the *T6-33* mutant line. ABI1 belongs to PP2Cs that inhibit OST1 function and are negative regulators of ABA-signalling pathway (Gosti et al., 1999; Fujii et al., 2009). It has been proposed that stomatal closure triggered by ABA or elevated CO_2 concentrations are intertwined, but the exact convergence point has not been ascertained yet (Hsu et al., 2018). At first, it was reported by Webb and Hetherington (1997) that the PP2Cs ABI1 and ABI2 might be the mediators in both signalling pathways. The gain-of-function mutation in ABI1 (*abi1-1*) results in the constant activity of this protein and lead to ABA-insensitivity, the mutant has more open stomata and reduced O_3 tolerance (Leung et al. 1994; Meyer et al. 1994; Jalakas et al., 2017). The changes in stomatal conductance in response to high CO_2 concentrations in this line are similar (Jalakas et al., 2017) or only slightly weaker compared to wild-type Col-0 (Merilo et al., 2013; Hsu et

al., 2018). Accordingly, it is unlikely that the impaired response to CO_2 stimulus in *T6-33* is caused by the mutation in *abi1-1*. Testing the response of *T6-33* mutant backcrosses to ABA could give clarification on whether ABI1 is involved in the emerged phenotype. Even if the ABI1 mutation is not relevant to CO_2 response in *T6-33* line, it could be responsible for the higher basal stomatal conductance of it. According to the yeast complementation test, the $AHA1^{L432F}$ is not associated with the phenotype development (Fig. 13). It is probable that neither of the mutations in the *T6-33* line is responsible for the plant phenotype and a new yet to be identified regulator is implicated.

To conclude, the point mutations in *SLAC1*, *ABI1* and *ABA4* could affect O_3-sensitive phenotypes and could be a reason for the selection of the AHA1 mutants in the large-scale mutant screen. The *G5/47A* mutant was affected by a point mutation in the SLAC1 region and no supplementary analysis is needed for this line in relation to AHA1 studies. Further backcrosses are needed for *G9/19C* and *T6-33* lines to eliminate the secondary mutations.

3.7. Generation of transgenic lines expressing AHA1 mutant variants

As indicated above, the amino acid substitutions in site G528 were picked more frequently than any other alterations in the AHA1 coding region. Moreover, we detected a substitution in M527, indicating that the amino acid residues at 527 and 528 position can play an important role in regulation of AHA1 activity. Due to the potential importance of this site for AHA1 regulation, we decided to study these substitutions in more detail. Previously, back-crosses with the *P34-32*, *G6/9D,* and *T6-34* mutants carrying these mutations (Table 5) have been initiated by M. Nuhkat and homozygous backcrossed plants were available before the start of this work.

In order to provide further insight for AHA1 regulation, we generated transgenic lines expressing AHA1 proteins with M527I, G528E, and G528R amino acid substitutions. The constructs for plant transformation were based on the pMLBart vector (Gleave, 1992) that has been proven to work successfully for *Arabidopsis* genetic transformation (Yarmolinsky et al., 2013). Cloned AHA1 cDNA sequence was modified by using the QuickChange site-directed mutagenesis technique to introduce the M527I, G528E, and G528R mutations. In the T-DNA region of pMLBart, mutated and wild-type AHA1 variants were expressed under the control of the native AHA1 promoter to ensure wild-type levels of transgene expression. Plasmids for plant transformation also contained expression cassettes for pH-GFP under the

control of guard cell-active SLAC1 promoter and the *BAR* gene for selection of transgenic plants on glufosinate (Basta). The empty control vector contained only pSLAC1::pH-GFP and the cassette for BAR expression. All constructs were introduced into *A. tumefaciens* strains which were used for *Arabidopsis* transformation.

As a genetic background for transgenic lines, an AHA1 knockdown line *aha1-6* was employed (Alonso et al., 2003). This mutant was obtained from the SALK transgenic plant collection and contains a T-DNA insertion in the AHA1 promoter. Similar to other single *aha1/2* loss-of-function mutants, *aha1-6* has no visible phenotype under laboratory conditions (Haruta et al., 2010). Despite the T-DNA insertion in the close vicinity to the AHA1 coding sequence, the *aha1-6* mutant still expresses low levels of AHA1 protein according to Haruta et al. (2010). Since a complete AHA1 knockout mutant was not available at the beginning of the studies, we used *aha1-6* for generating transgenic lines. The empty vector containing only pH-GFP was used for genetic transformation of Col-0, *ost2-2D* and *aha1-6* lines to generate needed control lines for comparisons.

3.8. Selection of transgenic lines

The transformation efficiency of the floral dip method is around 1% (Zhang et al., 2006) and, therefore, some methods are necessary to select plants that have acquired a plasmid. In this study, we developed transgenic plants that were resistant to herbicide glufosinate and contained the fluorescent protein pH-GFP, which was available in our laboratory.

The pH-GFP, also known as ratiometric pHluorin, is a pH-sensitive fluorescent reporter that was designed for measurements of changing pH values in a pH range between 5.5 and 7.5 (Miesenböck et al., 1998; Moyseko and Feldman, 2001). This range covers the proton gradient generated by plant H^+-ATPases – apoplastic and cytoplasmic pH values are 5-6 and 7, respectively (Palgmren, 2001). Therefore, pH-GFP is suitable to study H^+-ATPases in guard cells where AHA1 is expressed (Palmgren, 2001). To facilitate studies of guard cells, the pH-GFP gene was expressed under the control of the SLAC1 promoter known to be active in guard cells (Mustilli et al., 2002; Vahisalu et al., 2008). Activation of AHA1 should lead to additional acidification of the apoplast while the guard cell cytoplasm would become more alkaline (Moyseko and Feldman, 2001; Merlot et al., 2007). The pH-GFP protein is a ratiometric sensor with the excitation at 395 nm and 475nm and the emission maximum at 509 nm. Upon acidification, excitation at 395 nm decreases while excitation at 475 nm is

elevated, allowing to study cellular pH values by the 395/475nm emission ratio (Miesenböck et al., 1998).

Transgenic T1 seedlings were selected after sprays with Basta (glufosinate) solutions. Transgenic plants remained healthy after Basta sprays while plants without a transgene inserts withered and died. Plants that survived were labelled and their leaves were examined under a confocal microscope to assess the expression intensity of pH-GFP. For confocal microscopy, 405 and 488 nm lasers were selected based on the microscope technical capabilities to be close to the excitation maximums of pH-GFP.

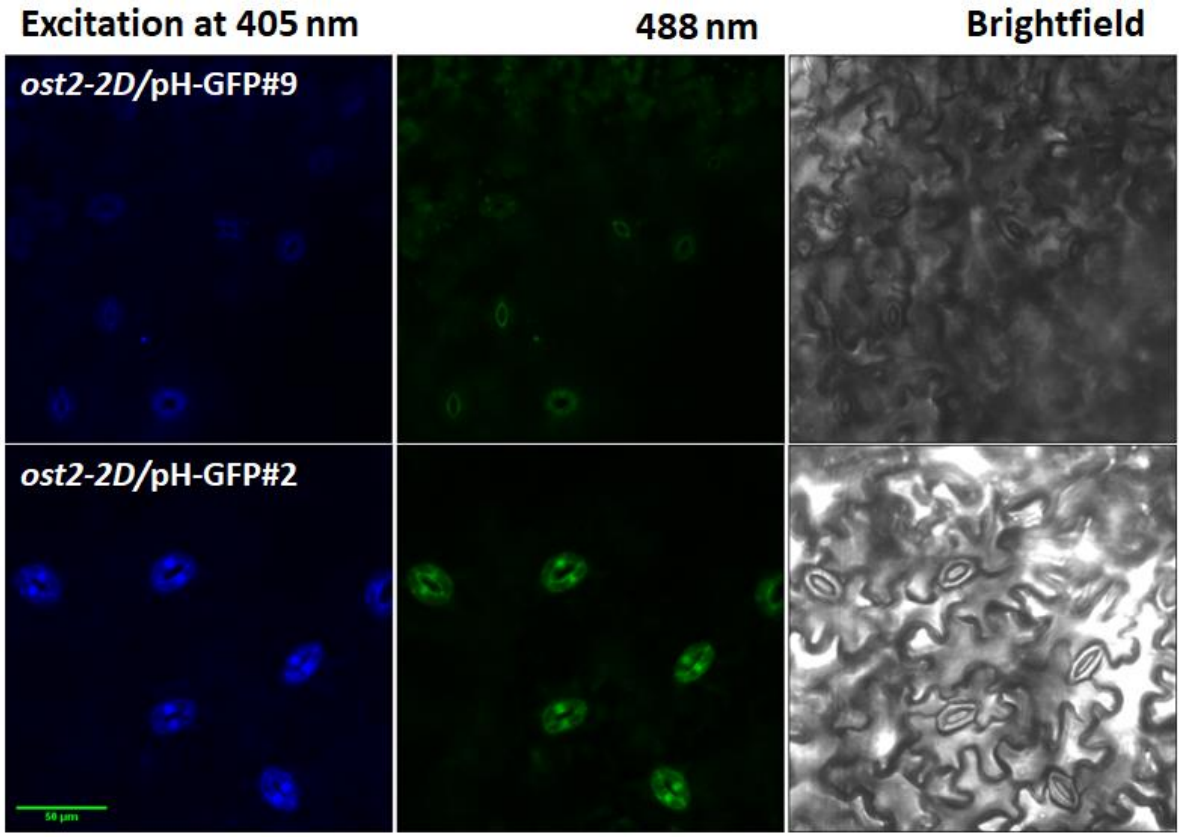

Figure 17. Detection of fluorescence in guard cells of *ost2-2D* transgenic lines carrying pH-GFP. The 405 and 488 beams were used to excite pH-GFP and fluorescence signal was detected in the range of 510-540 nm under LSM 710 META Laser Scanning Microscope. Also, the corresponding brightfield pictures are presented. The best transgenic lines for further research were selected based on the intensity of fluorescence signal, quantified using the Fiji software. The subline 9 of the *ost2-2D/pH-GFP* line showed only weak autofluorescence, while the subline 5 displayed a strong emission of pH-GFP. The scale bar corresponds to 50 µm.

The confocal imaging proved that the pH-GFP signals were detectable in guard cells (Fig. 15). The pH-GFP was expressed in the cytoplasm and the nuclei of guard cells. The penetration through the nuclear membrane had been already shown before for cytoplasmic pH-GFP (Moyseko and Feldman, 2001). The majority of plants exhibited pH-GFP fluorescence, but in

some of the transgenic plants the signal was extremely weak and close to the autofluorescence of the cell walls in stomata (Fig. 17).

Lines expressing pH-GFP at sufficient levels could be later examined for fluorescence ratio intensities in guard cells between excitation at 405 nm and 488 nm after background subtraction. As a result of higher proton extrusion from guard cells in case of constantly active AHA1, the expected ratio of 405/488 nm should be increased compared to Col-0 and YC3.6 plants. If this method turns out successful, this data could be used to speed up the selection process.

For further studies, 10 transgenic sublines with sufficient expression of pH-GFP were selected for each of the lines. The independent transgenic lines were designated according to their sequence number in the fluorescence imaging. To reduce the number of selected sublines, we estimated their water loss from detached leaves as the *ost2* mutants exhibit significantly higher water than wild-type plants (Merlot et al., 2007; Nuhkat, 2013). Preliminary experiments showed that the newly-discovered AHA1 mutants also demonstrated high steady-state stomatal conductance and enhanced water loss from leaves. T2 plants were grown and after treatments with Basta their water loss was studied to select sublines for gas exchange experiments. Col-0, *ost2-2D*, *ghr1-3* and *slac1-4* were used as control lines. The *ost2-2D* was chosen as a known AHA1 mutant in the Col-0 background (Merlot et al., 2002). The *ghr1-3* and *slac1*-4 mutants were employed as positive controls in the assays due to their high water loss.

Detached leaves of *ghr1-3* mutant show approximately 60% fresh weight loss after 2 hours of air-drying (Hua et al., 2012), while *slac1-4* has this parameter even about 75% (Vahisalu et al., 2008). These data are close to our results obtained herein (~60% and ~70%, respectively) (Fig. 18). The *ost2-2D* water loss was evaluated to be ~50%, more than 2 folds higher than that of wild-type Col-0 (22%). Surprisingly, Col-0/pH-GFP and *aha1-6/*pH-GFP lines exhibited approximately 8% higher water loss compared to Col-0, indicating that pH-GFP could influence stomatal functioning. The higher water loss could have also been caused by spraying the plants with BASTA. Similarly, water loss was also elevated in the *aha1-6* transgenic lines expressing wild-type AHA1. None of the mutated AHA1 transgenic lines showed as high average water loss as the *ost2-2D* mutant. Since Basta-treated T2 plants segregate homozygous: heterozygous plants as 1:2, we observed high variation in water loss

of individual transgenic plants expressing mutated AHA1 variants. Two of the AHA1^{G528E} transgenic lines demonstrated average water loss close to 50%. Individual transgenic plants from each mutated AHA1 line had water loss close to that in *ost2-2D*. The independent lines of AHA1^{M528I} and AHA1^{G528R} showed slightly enhanced water loss, but were rather closer to numbers obtained for wild-type Col-0 or Col-0/pH-GFP. Still some individual transgenic plants had enhanced water loss and these lines were selected for further gas exchange experiments.

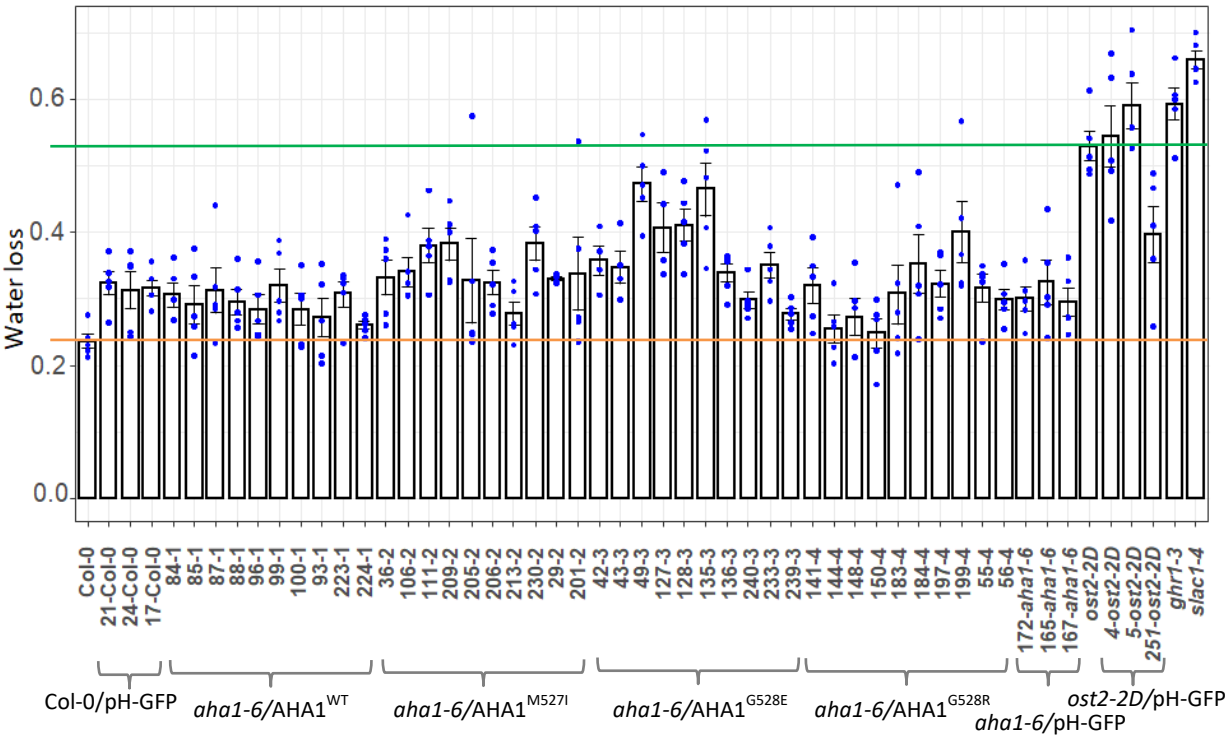

Figure 18. Water loss for selection of transgenic lines. Water loss of five plants from each subline was measured. The blue dots indicate values of water loss for individual plants. Orange strip denotes the level of WT Col-0 water loss, green one the same rate of *ost2-2D*. The values are mean ±SEM (n=5).

3.9. AHA1^{M527I}, AHA1^{G528E}, and AHA1^{G528R} result in impaired response to elevated CO_2

For a more detailed study, the phenotypes of transgenic lines were examined using time-resolved gas exchange measurements (Kollist et al., 2007). For preliminary experiments, T2 plants were grown and sprayed with Basta to select transgenic plants. Then, by using the gas exchange device, the steady-state stomatal conductance and response to high CO_2 of intact plants were determined. Stomatal closure in elevated CO_2 was induced by increasing the CO_2 concentration from ~400 ppm to ~800 ppm. Homozygous backcrossed EMS mutants were used as controls to select most promising transgenic lines. We used a set of 6 independent sublines with the highest water loss for each transgenic line expressing mutated AHA1

variants. In addition, two lines from every transgenic Col-0, *aha1-6* and *ost2-2D* and 5 of containing wild-type AHA1 construct were chosen considering the approximate water loss values in these lines. Results with most promising independent sublines are presented in Fig. 19.

As expected, *ost2-2D/*pH-GFP mutant did not respond to the elevation of CO_2 concentration as shown in the master thesis of M. Nuhkat (2013). Additionally, the backcrossed homozygous *P34-32*, *T6-34* and *G6/9D* mutants clearly exhibited an abolished response to elevated CO_2 (Fig. 19), which confirms the transmission of the AHA1-related phenotype to the next generation. The steady-state stomatal conductance of the *P34-32* and *T6-34* mutants (Fig. 19B, D) were also markedly higher compared with the controls (~120 mmol m^{-2} s^{-1} for YC3.6 and *aha1-6*/pH-GFP, and 150 mmol m^{-2} s^{-1} for Col-0/pH-GFP), reaching up to ~250 mmol m^{-2} s^{-1}, but being still lower than *ost2-2D/*pH-GFP values. The *G6/9D* mutant exhibited only a slight increase in stomatal conductance values compared with the controls and was the only F2 generation mutant showing a small 5% reduction in stomatal conductance in response to high CO_2 (Fig. 19C).

No difference between stomatal conductance in *aha1-6* and Col-0 wild-type plants was previously described (Yan et al., 2015). However, in our hands, the *aha1-6* transgenic line exhibit considerably lower values of stomatal conductance than Col-0 with pH-GFP control vector as well as with the AHA1 wild-type transgene (Fig 19A). The *aha1-6/*pH-GFP plants had the same level of stomatal conductance as YC3.6 which is known to have Col-0-like stomatal conductance (Sierla et al., 2018). Taken together, pSLAC::pH-GFP transgene could have an effect on stomatal conductance values. This is also confirmed by the fact that the water loss of transgenic plants was noticeably increased compared to wild-type Col-0 (Fig. 18). However, the response to CO_2 seemed to remain identical in those 4 lines, as their stomatal conductance decrease fell in the range 35-40%.

This information still allowed us to examine the phenotypes of transgenic lines that carry potentially gain-of-function AHA1 variants and to confirm that the transformation process was successful. The response to high CO_2 treatment differed between independent AHA1 transgenic lines, referring the expression of a transgene could vary from line to line (all data not shown; Fig. 19), which also was observed during the pH-GFP fluorescence imaging. At the same time, all three mutations in AHA1 transgenes were able to affect the

responsiveness to applied elevated CO_2 (Fig. 19). There was also detectable variation among the steady-state stomatal conductance values – some single plants displayed the values similar to F2 generation mutant lines that could have also represented the homozygous plants. However, mostly the rates of stomatal conductances remained at the level of Col-0 in transgenic lines.

From each transgenic line carrying AHA1 variants, one most promising independent line was selected taking into consideration every selection stage. Besides, the ratio of Basta-resistant to Basta-sensitive was estimated to limit T-DNA insertions in lines to one. The gas exchange results of chosen lines in response to CO_2 elevation have been presented showing every measured plant separately (Fig. 19B, C and D). For transgenic AHA1^{M527I} lines, the transgene could not restore the initial F2 generation stomatal conductance, whereas responses to increased CO_2 concentrations resembled those of *P34-32* F2 generation (Fig. 19B). 233-AHA1^{G528E} was showing more similarity to corresponding *G6/9D* screen background mutant, having only 8% lower average stomatal conductance after application of elevated CO_2 (Fig. 19C). On the contrary to the previous two lines, the average stomatal conductance of the transgenic 199-AHA1^{G528R} was clearly higher, having also a ~40% ascent from transgenic *aha1-6*/pH-GFP (Fig. 19D). However, in this case, the monitored reaction extent to CO_2 was greater than that of *T6-34* mutant, though the decline seemed decelerated compared to *aha1-6*/pH-GFP and YC3.6.

The variation in the steady-state stomatal conductance values and responses to CO_2 of transgenic lines may have also been caused due to a different expression level of native AHA1 in those plants, as the background mutant *aha1-6* is capable of expressing some of the protein (Haruta et al., 2010). In general, it is possible to conclude that the transformation worked for these different AHA1 lines and the method can be employed later for other AHA1 variants. However, further crosses must be performed with the most promising lines to avoid unwanted mutations that may have occurred during the transformation.

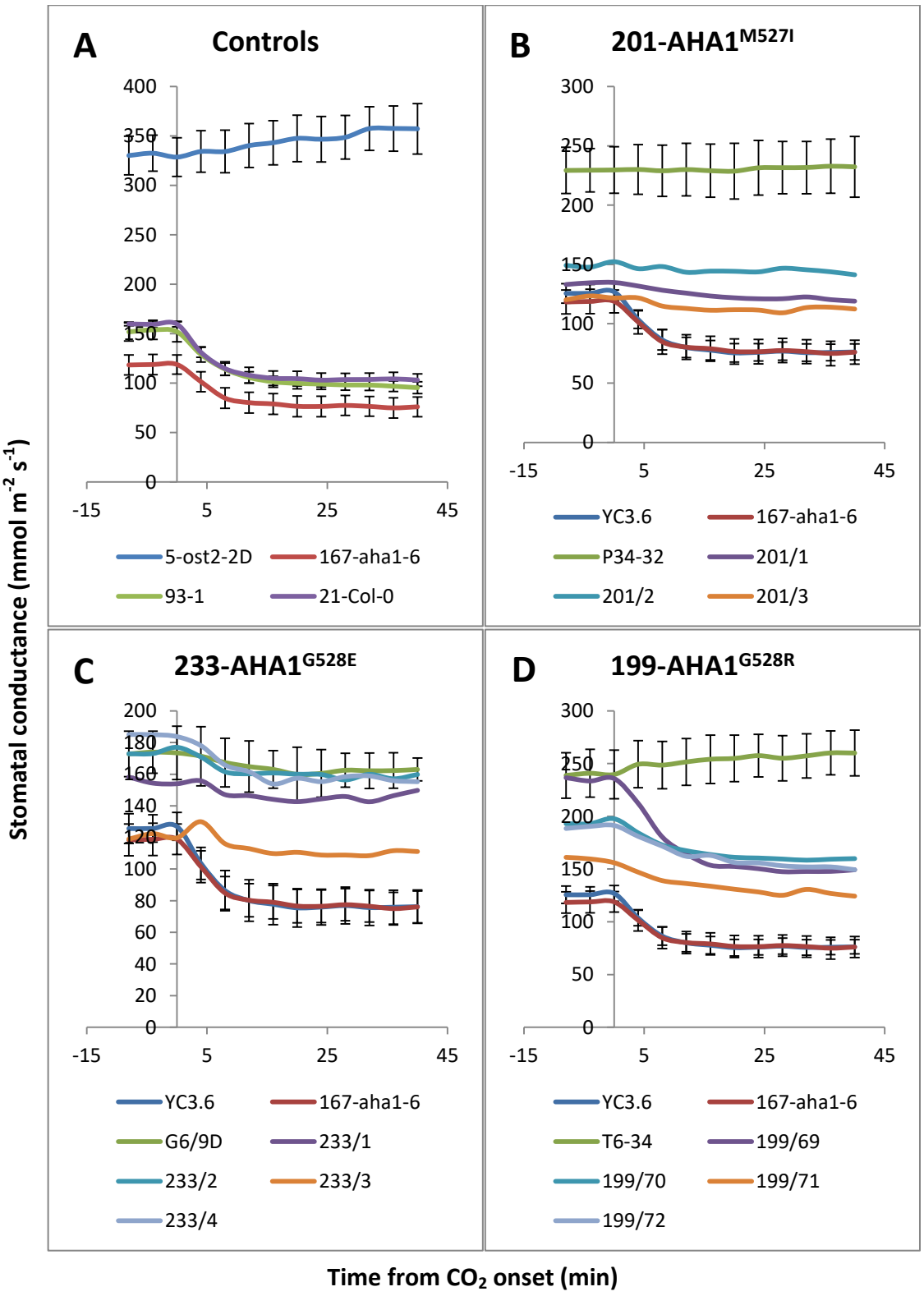

Figure 19. High CO_2 induced stomatal closure in the transgenic lines expressing wild-type and mutated variants of AHA1. Graphs represent the time-resolved stomatal conductance measurements, where high CO_2 (elevation of CO_2 concentration from 400 to 800 ppm) was applied at time point 0. The values are mean ±SEM (n=6-8).

3.10. Conclusions

All together we have tested 13 mutants with different newly-identified AHA1 mutations to determine whether they are responsible for the emerged mutant phenotypes. Based on the previous data and the results obtained within this thesis, we could confirm a few cases where these mutations are the main suspects for resulting phenotypes.

As for the L432F, E622K or R773K mutations in AHA1, the occurring alterations were not able to complement the yeast proton pump and could be silent mutations in the AHA1 coding region (Fig. 13). The certain phenotype of plants carrying these mutations could be explained by other mutations in the *Arabidopsis* genome. For example, it was ascertained that the phenotype of a line carrying E622K mutation in AHA1 was actually affected by the $SLAC1^{G313E}$ mutation (chapter 3.6). Interestingly, the F1 backcross of the *T6-33* mutant carrying L432F mutation still displayed severely impaired CO_2-induced stomatal closure and seemingly the accompanying mutation in ABI1 did not affect the plant growth. These results further emphasize that an entirely new stomatal regulator may cause the stomatal phenotype in this line. $AHA1^{R773K}$-containing *G8/39D* mutant line was initially identified as a relatively weak mutant and in following experiment showed a very similar to YC3.6 responsiveness to high CO_2 stimulus in the F1 backcross (Table 6). The subtle stomatal phenotype in the original *G8/39D* line might be caused by a combination of several minor mutations. Also, the $AHA1^{A876S}$ showed very weak complementation in the yeasts (Fig. 13) and plants with this mutation were not defective in high CO_2-triggered stomatal closure (Table 6), suggesting this substitution also displays minor significance to AHA1 functioning.

Experiments with mutants carrying A76T, A97M and G195L changes in AHA1 must be continued in order to obtain more information about these plant lines. Although based on the yeast complementation and F1 backcross generation results, the mutation A76T may represent a first described recessive allele of the AHA1 locus (Fig. 13; Table 6).

Among the most promising lines are the lines carrying mutations M527I, G528E and G528R in AHA1. As described above, these mutations showed some growth in yeast complementation assay (Fig. 13), the trait was carried over to the F2 generation of backcrossed initial mutants (Fig. 19). Furthermore, these mutations clearly affected the stomatal response to high CO_2 in created transgenic lines (Fig.19). The L919 site is part of the II autoinhibitory region in the AHA2 R-domain and was already described to potentially

regulate the AHA1 activity by Axelsen et al. (1999) and now also by Nguyen et al. (2020). The mutation A500T seems intriguing, as being one of the most efficient in yeasts (Fig. 13) and being able to show unresponsiveness to high CO_2 (Fig. 14C) in the F1 backcross. Although a bit less active in yeasts compared to A500T, the D165N is also possibly affecting the AHA1 activity and can show very clear impairment to high CO_2 in the backcrossed F1 generation. These two latter mutations could be further tested in respective transgenic plants.

Based on the speculations originated from Pedersen et al. (2007) findings, only the A-domain was thought to attach the regulatory R-domain. However, the latest view about AHAs has been proposed a mechanism where the R-domain crosslinks extensively in addition with sites in the P- and N-domains to regulate the catalytic cycle (Nguyen et al., 2020). In other words, these intramolecular bindings are considered to modulate the relative positions of the domains and, thus, regulate the proton efflux. With this in mind, the lines carrying AHA1 mutations M527I, G528E, G528R, A500T and D165N could be responsible for the R-domain attachment in their locations in P- and A-domains. Several binding sites in different domains could also explain why the complementation in yeast assays is not absolute in those sites like complete deletion of the R-domain, because their function may be divided. These five new mutations in AHA1 could give information in the future how the R-domain interacts with other domains and about the possible configurational changes of the AHA1 proton pump during transition between the two activity states.

SUMMARY

Although the crystal structure of proton pumps is known, decades of research have failed to determine the regulation details of these pumps in plants. In the large-scale screen for stomatal regulators, 13 mutants with newly-identified AHA1 point mutations were isolated that could shed light on those questions. The preliminary tests with these mutants demonstrated that the majority of these were not able to close their stomata in response to high CO_2.

To reduce the number of secondary mutations in the EMS mutagenized mutants and to confirm the AHA1 involvement in the resulting stomatal phenotype, the backcrosses were initiated with most of the lines. Some of the F1 generation backcrosses were performed within the framework of this Master's thesis as others had been done before. All backcrossed plants were studied in the gas exchange measurements using high CO_2 application. The results indicate that the majority of the causal mutations in these lines were dominant or semi-dominant since the response to elevated CO_2 in the F1 generation was still affected. We also generated transgenic lines with the most promising $AHA1^{M527I}$, $AHA1^{G528E}$, and $AHA1^{G528R}$ mutations and studied their phenotype using the gas exchange device. The CO_2 response in the generated lines was clearly affected, suggesting these mutation indeed are important for AHA1 functioning. Hence, the implemented method was successful and could be employed to study other AHA1 mutations.

Moreover, all gas exchange results were juxtaposed with data obtained from the yeast complementation assays to determine whether the tested AHA1 mutations could potentially be responsible for the emerged phenotype. In most cases, AHA1 mutations were able to rescue the yeast growth and, thus, can have an effect on plant growth. Those AHA1 mutations not active in yeast complementation tests denote silent mutations and the resulting plant phenotype could be explained by other mutations in the *Arabidopsis* genome.

To conclude, studies with the newly-identified AHA1 mutants will be continued to reduce the number of unwanted mutations in these lines. This method, together with the transgenic approach to transfer AHA1 variants carrying these mutations are needed to characterize. The newly-identified mutations could give us information about how the AHA1 activity is regulated under different environmental conditions.

RESÜMEE

Plasmamembraani prootonpumba AHA1 mutantide analüüs

Jaanika Unt

Kokkuvõte

Õhulõhed on kahest sulgrakust koosnevad poorid taimede lehtedel ja noortel vartel, mis vahendavad taimede gaasivahetust atmosfääriga. Õhulõhede kaudu siseneb taimedesse fotosünteesiks vajalik CO_2 ja väljub transpiratsiooni käigus veeaur. Erinevates keskkonnatingimustes on õhulõhede avatus reguleeritud sulgrakkudes toimuva turgorrõhu muutuste läbi. Õhulõhede avanemisel kogunevad sulgrakkudesse osmootselt aktiivsed ained ning sulgumisel nende kontsentratsioon väheneb. Ioonide ja vee sisenemine rakku õhulõhede avanemisel toimub plasmamembraani prootonpumpade poolt tekitatud energia arvelt. Samuti on näidatud prootonpumpade tähtsust õhulõhede sulgumisreaktsioonis. Ehkki prootonpumpade kristallstruktuur on teada, pole siiani selge, kuidas prootonpumpade tegevus taimedes on reguleeritud.

Nendele küsimustele võivad vastuse anda mutantsetes liinides hiljuti avastatud uued punktmutatsioonid AHA1 prootonpumbas, mis on üks peamisi plasmamembraani prootonpumpasi *Arabidopsis thaliana* õhulõhedes. Eksperimentaalne töö konkreetsete mutantidega näitasid, et kõrge CO_2 kontsentratsioonid korral on nende õhulõhede sulgumine häiritud. Tuvastatud AHA1 mutantidega viidi läbi tagasiristamised vanemliiniga, et vähendada mutageniseerimise käigus tekkinud sekundaarsete mutatsioonide arvu ja kinnitada AHA1 mutatsioonide seotust fenotüübi kujunemisel. Samuti loodi kolme kõige sagedamini detekteeritud mutatsiooniga transgeensed taimed. Tagasiristatud ning transgeensete taimede fenotüüpi uuriti gaasivahetuskatsetes rakendades neile kõrge CO_2 stiimulit. Saadud andmeid võrreldi pärmide komplementatsiooni testidega.

Tulemustest järeldus, et suurem osa mutatsioone konkreetsetes liinides on dominantsed või semi-dominantsed ning enamike taimede fenotüüp on seotud AHA1 mutatsioonidega. Siiski peaksid edasised katsed tooma selles osas täit selgust. Lisaks oli transgeensete liinide loomine edukas ning antud metoodikat võib rakendada ka edaspidi teiste AHA1 mutatsioonide uurimiseks.

ACKNOWLEDGMENTS

First of all, I would like to thank my supervisor Dmitry Yarmolinsky for his patience, calmness and persistence. I appreciate everything you did for me and how you saw opportunity where I no longer had much hope. I thank also Hannes Kollist for the chance to work in The Plant Signal research group and for the kind words during thesis writing.

Special thanks go to Mikk Välbe for being always present when something critical happened and help was desperately needed. And Helen, if there had not been long nights at the lab full of complaining about our hard times, I would probably have panicked at home and gone mad. I am grateful to my amazing office-mates Maris Nuhkat, Ashutosh Pandey and Chung-Yueh Yeh for the great atmosphere and their advice. Even if there was no one else around to see, at least one of you always greeted me in our small office and I did not have to feel lonely.

I would like to thank all the members of The Plant Signal Research Group for inspiring me and being such good companions throughout my studies.

Many thanks go to my dear friend Rein Leetmaa. You know exactly what and when to say to make me feel better. I am also thankful for the time you spent on giving me advice.

I am thankful also to my supportive parents. Last but not least – Andres, without your support I could not have done this. Thank you for being you, always understanding and caring.

REFERENCES

Ache, P., Becker, D., Ivashikina, N., Dietrich, P., Roelfsema, M.R.G. and Hedrich, R. (2000). GORK, a delayed outward rectifier expressed in guard cells of *Arabidopsis thaliana*, is a K^+-selective, K^+-sensing ion channel. FEBS Letters. 486: 93-8.

Ainsworth, E.A., Yendrek, C.R., Sitch, S., Collins, W.J. and Emberson, L.D. (2012). The effects of tropospheric ozone on net primary productivity and implications for climate change. Annu Rev Plant Biol. 63: 637-61.

Alonso, J.M., Stepanova, A.N., Leisse, T.J., … Ecker, J.R. (2003). Genome-wide insertional mutagenesis of *Arabidopsis thaliana*. Science. 301(5633): 653-7.

Axelsen, K.B. and Palmgren, M.G. (2001). Inventory of the superfamily of P-Type ion pumps in *Arabidopsis*. Plant Physiol. 126(2): 696-706.

Axelsen, K.B., Venema, K., Jahn, T., Baunsgaard, L. and Palmgren, M.G. (1999). Molecular dissection of the C-terminal regulatory domain of the plant plasma membrane H^+-ATPase AHA2: mapping of residues that when altered give rise to an activated enzyme. Biochemistry. 38(22): 7227-34.

Baxter, I., Tchieu, J., Sussman, M.R., Boutry, M., Palmgren, M.G., Gribskov, M., Harper, J.F. and Axelsen, K.B. (2003). Genomic comparison of P-type ATPase ion pumps in *Arabidopsis* and rice. Plant Physiol. 132: 618-28.

Buch-Pedersen, M.J. and Palmgren, M.G. (2003). Conserved Asp684 in transmembrane segment M6 of the plant plasma membrane P-type proton pump AHA2 is a molecular determinant of proton translocation. J Biol Chem. 278(20): 17845-51.

Buch-Pedersen, M.J. and Palmgren, M.G. (2003). Mechanism of proton transport by plant plasma membrane proton ATPases. J Plant Res. 116(6): 507-15.

Cid, A., Perona, R. and Serrano, R. (1987) Replacement of the promoter of the yeast plasma membrane ATPase gene by a galactose-dependent promoter and its physiological consequences. Curr Genet. 12: 105-10.

Clough, S.J. and Bent, A.F. (1998). Floral dip: a simplified method for *Agrobacterium*-mediated transformation of *Arabidopsis thaliana*. Plant J. 16: 735-43.

Dall'Osto, L., Cazzaniga, S., North, H., Marion-Poll, A. and Bassia, R. (2007). The *Arabidopsis aba4-1* mutant reveals a specific function for neoxanthin in potection against photooxidative stress. Plant Cell. 19(3): 1048-64.

Daszkowska-Golec, A. and Szarejko, I. (2013). Open or close the gate – stomata action under the control of phytohormones in drought stress conditions. Front Plant Sci. 4: 138.

Duby, G. and Boutry, M. (2009). The plant plasma membrane proton pump ATPase: a highly regulated P-type ATPase with multiple physiological roles. Pflugers Arch. 457(3): 645-55.

Edwards, A. and Bowling, D.J.F. (1985). Evidence for a CO_2 inhibited proton extrusion pump in the stomatal cells of *Tradescantia virginiana*. J Exp Bot. 36(162): 91-8.

Ekberg, K., Palmgren, M.G., Veierskov, B., Buch-Pedersen, M.J. (2010). A novel mechanism of P-type ATPase autoinhibition involving both termini of the protein. J Biol Chem. 285(10): 7344-50.

Falhof, J., Pedersen, J.T., Fuglsang, A.T. and Palmgren, M. (2016). Plasma membrane H(+)-ATPase regulation in the center of plant physiology. Mol Plant. 9(3): 323-37.

Finkelstein, R. (2013). Abscisic acid synthesis and response. *Arabidopsis* Book. 11: e0166.

Focht, D., Croll, T.I., Pedersen, B.P. and Nissen, P. (2017). Improved model of proton pump crystal structure obtained by interactive molecular dynamics flexible fitting expands the mechanistic model for proton translocation in P-Type ATPases. Front Physiol. 8(2): 202.

Fuglsang, A.T., Kristensen, A., Cuin, T.A., … Palmgren, M.G. (2014). Receptor kinase-mediated control of primary active proton pumping at the plasma membrane. Plant J. 80(6): 951-64.

Fujii, H., Chinnusamy, V., Rodrigues, A., Rubio, S., Antoni, R., Park, S.Y., Cutler, S.R., Sheen, J., Rodriguez, P.L. and Zhu J.K. (2009). *In vitro* reconstitution of an abscisic acid signalling pathway. Nature. 462(7273): 660-4.

Gaxiola, R.A., Palmgren, M.G. and Schumacher, K. (2007). Plant proton pumps. FEBS letters. 581(12): 2204-14.

Geiger, D., Maierhofer, T., Al-Rasheid, K.A., … Hedrich, R. (2011). Stomatal closure by fast abscisic acid signaling is mediated by the guard cell anion channel SLAH3 and the receptor RCAR1. Sci Signal. 4.

Gleave, A.P. (1992). A versatile binary vector system with a T-DNA organisational structure conducive to efficient integration of cloned DNA into the plant genome. Plant Mol Biol. 20(6): 1203-7.

Gosti, F., Beaudoin, N., Serizet, C., Webb, A.A.R., Vartanian, N. and Giraudat, J. (1999). ABI1 protein phosphatase 2C is a negative regulator of abscisic acid signaling. Plant Cell. 11(10): 1897-910.

Guo, F.-Q., Young, J. and Crawford, N.M. (2003). The nitrate transporter AtNRT1.1 (CHL1) functions in stomatal opening and contributes to drought susceptibility in *Arabidopsis*. Plant Cell. 15(1): 107-17.

Harper, J.F., Manney, L., DeWitt, N.D., Yoo, M.H. and Sussman, M.R. (1990). The *Arabidopsis thaliana* plasma membrane H(+)-ATPase multigene family. Genomic sequence and expression of a third isoform. J Biol Chem. 265(23): 13601-8.

Harper, J.F., Surowy, T.K. and Sussman, M.R. (1989). Molecular cloning and sequence of cDNA encoding the plasma membrane proton pump (H^+-ATPase) of *Arabidopsis thaliana*. Proc Natl Acad Sci U S A. 86(4): 1234-8.

Haruta, M., Burch, H.L., Nelson, R.B., Barrett-Wilt, G., Kline, K.G., Mohsin, S.B., Young, J.C., Otegui, M.S. and Sussman, M.R. (2010). Molecular characterization of mutant *Arabidopsis* plants with reduced plasma membrane proton pump activity. J Biol Chem. 285(23): 17918-29.

Haruta, M., Gray, W.M. and Sussman, M.R. (2015). Regulation of the plasma membrane proton pump (H^+-ATPase) by phosphorylation. Curr Opin Plant Biol. 28: 68-75.

Hashimoto-Sugimoto, M., Negi, J., Monda, K., Higaki, T., Isogai, Y., Nakano, T., Hasezawa, S. and Iba, K. (2016). Dominant and recessive mutations in the Raf-like kinase HT1 gene completely disrupt stomatal responses to CO_2 in *Arabidopsis*. J Exp Bot. 67: 3251-61.

Hayashi, M., Inoue, S.-I., Takahashi, K., Kinoshita T. (2011). Immunohistochemical detection of blue light-induced phosphorylation of the plasma membrane H^+-ATPase in stomatal guard cells. Plant Cell Physiol. 52: 1238-48.

Hopkin, M. (2007). Carbon sinks threatened by increasing ozone. Nature 448: 396-7.

Hõrak, H., Sierla, M., Tõldsepp, K., … Kollist, H. (2016). A dominant mutation in the HT1 kinase uncovers roles of MAP kinases and GHR1 in CO_2-induced stomatal closure. Plant Cell. 28: 2493-509.

Hsu, P.-K., Takahashi, Y., Munemasa, S., Merilo, E., Laanemets, K., Waadt, R., Pater, D., Kollist, H. and Shroeder, J.I. (2018). Abscisic acid-independent stomatal CO_2 signal transduction pathway and convergence of CO_2 and ABA signaling downstream of OST1 kinase.

Hu, H., Boisson-Dernier, A., Israelsson-Nordström, M., Böhmer, M., Xue, S., Ries, A., Godoski, J., Kuhn, J.M. and Schroeder, J.I. (2010). Carbonic anhydrases are upstream regulators in guard cells of CO_2-controlled stomatal movements. Nat Cell Biol. 12: 87-93.

Hua, D., Wang, C., He, J., Liao, H., Duan, Y., Zhu, Z., Guo, Y., Chen Z. and Gonga, Z. (2012). A plasma membrane receptor kinase, GHR1, mediates abscisic acid – and hydrogen peroxide-regulated stomatal movement in *Arabidopsis*. Plant Cell. 24(6): 2546-61.

IPCC. (2014). Climate Change 2014: Synthesis Report. Contribution of working Groups I, II and III to the fifth assessment report of the intergovernmental panel on climate change. Geneva, Switzerland.

Jahn, T., Fuglsang, A.T., Olsson, A., Brüntrup, I.M., Collinge, D. B., Volkmann, D., Sommarin, M., Palmgren, M.G. and Larsson, C. (1997). The 14-3-3 protein interacts directly with the C-terminal region of the plant plasma membrane H(+)-ATPase. Plant Cell. 9(10): 1805-14.

Jakobson, L., Vaahtera, L., Tõldsepp, K., … Brosche, M. (2016). Natural variation in *Arabidopsis* Cvi-0 accession reveals an important role of MPK12 in guard cell CO_2 signaling. PLoS Biol. 14: e2000322.

Jalakas, P., Huang, Y.-C., Yeh, Y.-H., Zimmerli, L., Merilo, E., Kollist, H. and Brosché, M. (2017). The role of ENHANCED RESPONSES TO ABA1 (ERA1) in *Arabidopsis* stomatal responses is beyond ABA signaling. Plant Physiol. 174(2): 665-71.

Jones, R.J. and Mansfield, T.A. (1970). Suppression of stomatal opening in leaves treated with abscisic acid. J exp Bot. 21: 714-9.

Jørgensen, P.L. and Andersen, J.P. (1988). Structural basis for E1-E2 conformational transitions in Na, K-pump and Ca-pump proteins. J Membr Biol. 103(2): 95-120.

Kanczewska, J., Marco, S., Vandermeeren, C., Maudoux, O., Rigaud, J.L. and Boutry, M. (2005). Activation of the plant plasma membrane H^+-ATPase by phosphorylation and binding of 14-3-3 proteins converts a dimer into a hexamer. Proc Natl Acad Sci U S A. 102: 11675-80.

Kinoshita, T. and Shimazaki, K. (2002). Biochemical evidence for the requirement of 14-3-3 protein binding in activation of the guard-cell plasma membrane H^+-ATPase by blue light. Plant Cell Physiol. 43: 1359-65.

Kollist, H., Nuhkat, M. and Roelfsema, M.R.G. (2014). Closing gaps: linking elements that control stomatal movement. New Phytol. 203(1): 44-62.

Konieczny, A. and Ausubel, F.M. (1993.) A procedure for mapping *Arabidopsis* mutations using co-dominant ecotype-specific PCR-based markers. Plant J. 4(2): 403-10.

Koornneef, M., Reuling, G. and Karssen, C.M. (1984). The isolation and characterization of abscisic acid-insensitive mutants of *Arabidopsis thaliana*. Physiol Plant. 61: 377-83.

Lee, M., Choi, Y., Burla, B., Kim, Y.Y., Jeon, B., Maeshima, M., Yoo, J.Y., Martinoia, E. and Lee, Y. (2008). The ABC transporter AtABCB14 is a malate importer and modulates stomatal response to CO_2. Nat Cell Biol. 10(10): 1217-23.

Lee, S.C., Lan, W., Buchanan, B B. and Luan, S. (2009). A protein kinase-phosphatase pair interacts with an ion channel to regulate ABA signaling in plant guard cells. Proc Natl Acad Sci U S A. 106(50): 21419-24.

Lesk, C., Rowhani, P. and Ramankutty, N. (2016). Influence of extreme weather disasters on global crop production. Nature. 529: 84-7.

Leung, J., Bouvier-Durand, M., Morris, P.C., Guerrier, D., Chefdor, F. and Giraudat, J. (1994). *Arabidopsis* ABA response gene ABI1: features of a calcium-modulated protein phosphatase. Science. 264(5164): 1448-52.

Liu, H. and Naismith, J.H. (2008). An efficient one-step site-directed deletion, insertion, single and multiple-site plasmid mutagenesis protocol. BMC Biotechnol. 8: 91.

Ma, Y., Szostkiewicz, I., Korte, A., Moes, D., Yang, Y., Christmann, A. and Grill, E. (2009). Regulators of PP2C phosphatase activity functions as abscisic acid sensors. Science. 324: 1064-8.

Merilo, E., Laanemets, K., Hu, H., ... Kollist, H. (2013). PYR/RCAR receptors contribute to ozone-, reduced air humidity-, darkness-, and CO_2-induced stomatal regulation. Plant Physiol. 162: 1652-68.

Merilo, E., Yarmolinsky, D., Jalakas, P., Parik, H,. Tulva, I., Rasulov, B.,Kilk, K. and Kollist, H. (2018). Stomatal VPD response: there is more to the story than ABA. Plant Physiol. 176(1): 851-64.

Merilo. E., Jalakas. P., Kollist. H. and Brosché, M. (2015). The role of ABA recycling and transporter proteins in rapid stomatal responses to reduced air humidity, elevated CO_2, and exogenous ABA. Mol Plant. 8: 657-9.

Merlot, S., Gosti, F., Guerrier, D., Vavasseur, A. and Giraudat J. 2001. The ABI1 and ABI2 protein phosphatases 2C act in a negative feedback regulatory loop of the abscisic acid signalling pathway. Plant J. 25(3): 295-303.

Merlot, S., Leonhardt, N., Fenzi, F., … Leung, J. (2007). Constitutive activation of a plasma membrane H^+-ATPase prevents abscisic acid-mediated stomatal closure. EMBO J. 26: 3216-26.

Merlot, S., Mustilli, A.-C., Genty, B., North, H., Lefebvre, V., Sotta, B., Vavasseur, A. and Giraudat, J. (2002). Use of infrared thermal imaging to isolate *Arabidopsis* mutants defective in stomatal regulation. Plant J. 30: 601-9.

Meyer, K., Leube, M.P., and Grill, E. (1994). A protein phosphatase 2C involved in ABA signal transduction in *Arabidopsis thaliana*. Science. 264(5164): 1452-55.

Meyer, S., Mumm, P., Imes, D., Endler, A., Weder, B., Al-Rasheid, K.A., Geiger, D., Marten, I., Martinoia, E. and Hedrich, R. (2010). AtALMT12 represents an R-type anion channel required for stomatal movement in *Arabidopsis* guard cells. Plant J. 63: 1054-62.

Miesenböck, G., De Angelis, D.A. and Rothman, J.E. (1998). Visualizing secretion and synaptic transmission with pH-sensitive green fluorescent proteins. Nature. 394(6689): 192-5.

Morsomme, P. and Boutry, M. (2000). The plant plasma membrane H(+)-ATPase: structure, function and regulation. Biochim Biophys Acta. 1465(1-2): 1-16.

Moseyko , N. and Feldman, L.J. (2001). Expression of pH-sensitive green fluorescent protein in *Arabidopsis thaliana*. Plant Cell Environ. 24(5): 557-63.

Negi, J., Matsuda, O., Nagasawa, T., Oba, Y., Takahashi, H., Kawai-Yamada, M., Uchimiya, H., Hashimoto, M. ja Iba, K. (2008). CO_2 regulator SLAC1 and its homologues are essential for anion homeostasis in plant cells. Nature. 452(7186): 483-6.

Nguyen, T.T., Blackburn, M.R. and Sussman, M.R. (2020). Inter- and intra-molecular interactions of the *Arabidopsis* plasma membrane proton pump revealed using a mass spectrometric-cleavable crosslinker. Biochemistry.

North, H.M., De Almeida, A., Boutin, J.-P., Frey, A., To, A., Botran, L., Sotta, B. and Marion-Poll, A. (2007). The *Arabidopsis* ABA-deficient mutant aba4 demonstrates that the major route for stress-induced ABA accumulation is via neoxanthin isomers. Plant J. 50(5): 810-24.

Nuhkat, M. (2013). Impaired stomatal closure: a case study of two types of *Arabidopsis* lines.

Ottmann, C., Marco, S., Jaspert, N., … Oecking, C. (2007). Structure of a 14-3-3 coordinated hexamer of the plant plasma membrane H^+-ATPase by combining X-ray crystallography and electron cryomicroscopy. Mol Cell. 25: 427-40.

Palmgren, M.G. (1991). Regulation of plant plasma membrane H^+-ATPase activity. Physiol Plant. 83: 314-23.

Palmgren, M.G. (2001). Plant plasma membrane H^+-ATPases: powerhouses for nutrient uptake. Annu Rev Plant Physiol Plant Mol Biol. 52: 817-45.

Palmgren, M.G. and Christensen, G. (1993). Complementation in situ of the yeast plasma membrane H(+)-ATPase gene pma1 by an H(+)-ATPase gene from a heterologous species. FEBS Lett. 317(3): 216-22.

Palmgren, M.G., Sommarin, M., Serrano, R. and Larsson, C. (1991). Identification of an autoinhibitory domain in the C-terminal region of the plant plasma membrane H(+)-ATPase. J Biol Chem. 266(30): 20470-5.

Pantin, F., Monnet, F., Jannaud, D., Costa, J.M., Renaud, J., Muller, B., Simonneau, T. and Genty, B. (2013). The dual effect of abscisic acid on stomata. New Phytol. 197(1): 65-72.

Park, S.Y., Fung, P., Nishimura, N., … Cutler, S.R. (2009). Abscisic acid inhibits type 2C protein phosphatases via the PYR/PYL family of START proteins. Science. 324: 1068-71.

Pedersen, B.P., Buch-Pedersen, M.J., Morth, J.P., Palmgren, M.G. and Nissen, P. (2007). Crystal structure of the plasma membrane proton pump. Nature. 450(7172): 1111-4.

Pedersen, P. and Carafoli, E. (1987). Ion motive ATPases: I. Ubiquity, properties, and significance to cell function. Trends Biochem Sci. 4: 146-50.

Pilot, G., Lacombe, B., Gaymard, F., Cherel, I., Boucherez, J., Thibaud, J.B. and Sentenac, H. (2001). Guard cell inward K^+ channel activity in *Arabidopsis* involves expression of the twin channel subunits KAT1 and KAT2. J Biol Chem. 276: 3215-21.

Raschke, K. (1975). Simultaneous requirement of carbon dioxide and abscisic acid for stomatal closing in *Xanthium strumarium L*. Planta. 125: 243-59.

Regenberg, B., Villalba, J.M., Lanfermeijer, F.C. and Palmgren, M.G. (1995). C-terminal deletion analysis of plant plasma membrane H(+)-ATPase: yeast as a model system for solute transport across the plant plasma membrane. Plant Cell. 7(10): 1655-66.

Roelfsema, M.R.G. and Hedrich, R. (2005). In the light of stomatal opening: new insights into 'the Watergate'. New Phytol. 167(3): 665-91.

Rudashevskaya, E.L., Ye, J., Jensen, O.N., Fuglsang, A.T. and Palmgren, M.G. (2012). Phosphosite mapping of P-type plasma membrane H^+-ATPase in homologous and heterologous environments. J Biol Chem. 287(7): 4904-13.

Schachtman, D.P., Schroeder, J.I., Lucas, W.J., Anderson, J.A. and Gaber, R.F. (1992). Expression of an inward-rectifying potassium channel by the *Arabidopsis* KAT1 cDNA. Science. 258(5088): 1654-8.

Schroeder, J.I. and Keller, B.U. (1992). Two types of anion channel currents in guard cells with distinct voltage regulation. Proc Natl Acad Sci U S A. 89(11): 5025-9.

Sharkey, T.D. and Raschke, K. (1981). Effect of light quality on stomatal opening in leaves of *Xanthium strumarium L*. Plant Physiol. 68(5): 1170-4.

Shimazaki, K., Doi, M., Assmann, S.M. and Kinoshita T. (2007). Light regulation of stomatal movement. Annu Rev Plant Biol. 58: 219-47.

Sierla, M., Hõrak, H., Overmyer, K., … Kangasjärvi, J. (2018). The receptor-like pseudokinase GHR1 is required for stomatal closure. Plant Cell. 30(11): 2813-37.

Sussman, M.R. (1994). Molecular analysis of proteins in the plant plasma membrane. Annu Rev Plant Physiol Plant Mol Biol. 45: 211-34.

Sussman, M.R. and Harper, J.F. (1989). Molecular biology of the plasma membrane of higher plants. Plant Cell. 1(10): 953-60.

Svennelid, F., Olsson, A., Piotrowski, M., Rosenquist, M., Ottman, C., Larsson, C., Oecking, C. and Sommarin, M. (1999). Phosphorylation of Thr-948 at the C terminus of the plasma membrane H(+)-ATPase creates a binding site for the regulatory 14-3-3 protein. Plant Cell. 11(12): 2379-91.

Sze, H. (1985). H^+-translocating ATPases: advances using membrane vesicles. Annu Rev Plant Physiol Plant Mol Biol. 36: 175-208.

Szyroki, A., Ivashikina, N., Dietrich, P., … Hedrich, R. (2001). KAT1 is not essential for stomatal opening. Proc Natl Acad Sci USA. 98: 2917-21.

Trejo, C.L., Davies, W.J. and Ruiz, L. de M.P. (1993). Sensitivity of stomata to abscisic acid: an effect of the mesophyll. Plant Physiol. 102: 497-502.

Ueno, K., Kinoshita, T., Inoue, S., Emi, T. and Shimazaki, K. (2005). Biochemical characterization of plasma membrane H^+-ATPase activation in guard cell protoplasts of *Arabidopsis thaliana* in response to blue light. Plant Cell Physiol. 46: 955-63.

Umezawa, T., Sugiyama, N., Mizoguchi, M., Hayashi, S., Myouga, F., Yamaguchi-Shinozaki, K., Ishihama, Y., Hirayama, T. and Shinozaki, K. (2009). Type 2C protein phosphatases directly

regulate abscisic acid-activated protein kinases in *Arabidopsis*. Proc Natl Acad Sci U S A. 106(41): 17588-93.

Unt, J. (2018). Õhulõhede regulatsiooni uurimine epidermise lõikude ja gaasivahetusmeetodite võrdluses harilikus müürloogas abstsiishappe toimel.

Vahisalu, T., Kollist, H., Wang, Y.F., … Kangasjärvi, J. (2008). SLAC1 is required for plant guard cell S-type anion channel function in stomatal signalling. Nature. 452(7186): 467-91.

Villalba, J., Palmgren, M., Berberian, G., Ferguson, G. and Serrano, R. (1992). Functional expression of plant plasma membrane H^+-ATPase in yeast endoplasmic reticulum. J Biol Chem. 267: 12341-9.

Waggoner, P.E. and Zelitch, I. (1965). Transpiration and the stomata of leaves. Science. 150(3702): 1413-20.

Wang, C., Hu, H., Qin, X., Zeise, B., Xu, D., Rappel, W.-J., Boron, W.F. and Schroeder, J.I. (2016). Reconstitution of CO_2 regulation of SLAC1 anion channel and function of CO_2-permeable PIP2;1 aquaporin as CARBONIC ANHYDRASE4 interactor. Plant Cell. 28: 568-82.

Waszczak, C., Vahisalu, T., Yarmolinsky, D., … Kangasjärvi J. (unpublished). Genetic screen to saturate guard cell signaling network reveals a role of GDP-L-fucose metabolism in stomatal closure. Plant Cell.

Webb, A.A. and Hetherington, A.M. (1997). Convergence of the abscisic acid, CO_2, and extracellular calcium signal transduction pathways in stomatal guard cells. Plant Physiol. 114: 1557-60.

Weigel, D and Glazebrook, J. (2008). Genetic analysis of *Arabidopsis* mutants. CSH Protoc. 3(2008): pdb.top35.

Weigel, D. and Glazebrook, J. (2009). Quick miniprep for plant DNA isolation. Cold Spring Harb Protoc. 2009(3): pdb.prot5179.

Willmer, C. and Ficker, M. 1996. Stomata, 2nd ed. Chapmand & Hall. London, UK.

Xue, S., Hu, H., Ries, A., Merilo, E., Kollist, H. and Schroeder, J.I. (2011). Central functions of bicarbonate in S-type anion channel activation and OST1 protein kinase in CO_2 signal transduction in guard cell. EMBO J. 30: 1645-58.

Yamamoto, Y., Negi, J., Wang, C., Isogai, Y., Schroeder, J.I. and Ibaa, K. (2016). The transmembrane region of guard cell SLAC1 channels perceives CO_2 signals via an ABA-independent pathway in *Arabidopsis*. Plant Cell. 28(2): 557-67.

Yan, S., McLamore, E.S., Dong, S., Gao, H., Taguchi, M., Wang, N., Zhang, T., Su, X. and Shen, Y. (2015). The role of plasma membrane H(+)-ATPase in jasmonate-induced ion fluxes and stomatal closure in *Arabidopsis thaliana*. Plant J. 83(4): 638-49.

Yang, Y., Costa, A., Leonhardt, N., Siegel, R.S. and Schroeder, J.I. (2008). Isolation of a strong *Arabidopsis* guard cell promoter and its potential as a research tool. Plant Methods. 4: 6.

Yarmolinsky, D., Brychkova, G., Fluhr, R. and Sagi M. Sulfite reductase protects plants against sulfite toxicity. (2013). Plant Physiol. 161(2): 725-43.

Zhang, J., De-Oliveira-Ceciliato, P., Takahashi, … Schroeder, J.I. (2018). Insights into the molecular mechanisms of CO_2-mediated regulation of stomatal movements. Curr Biol. 28(23): R1356-63.

Zhang, J., Wang, N., Miao, Y., Hauser, F., McCammon, J.A., Rappel, W.J. and Schroeder, J.I. (2018). Identification of SLAC1 anion channel residues required for CO_2/bicarbonate sensing and regulation of stomatal movements. Proc Natl Acad Sci U S A. 115(44): 11129-37.

Zhang, X., Henriques, R., Lin, S.-S., Niu, Q.-W. and Chua, N.-H. (2006). *Agrobacterium*-mediated transformation of *Arabidopsis thaliana* using the floral dip method. Nat Protoc. . 1(2): 641-6.

Used web addresses:

Benchling: https://www.benchling.com/

BlastDigester: http://bar.utoronto.ca/ntools/cgi-bin/ntools_blast_digester.cgi (28.02.2020)

QuickChange Primer Design Program:
https://www.agilent.com/store/primerDesignProgram.jsp?toggle=uploadTrans&mutate=true&_requestid=95605 (28.05.2020)

TAIR: The Arabidopsis Information Resource**,** http://www.arabidopsis.org/

NON-EXCLUSIVE LICENCE

I, Jaanika Unt,

1. herewith grant the University of Tartu a free permit (non-exclusive licence) to:

1.1. reproduce, for the purpose of preservation, including for adding to the DSpace digital archives until the expiry of the term of copyright, and

1.2. make available to the public via the web environment of the University of Tartu, including via the DSpace digital archives, under the Creative Commons licence CC BY NC ND 3.0, which allows, by giving appropriate credit to the author, to reproduce, distribute the work and communicate it to the public, and prohibits the creation of derivative works and any commercial use of the work from **12/06/2023** until the expiry of the term of copyright,

Characterization of plasma membrane proton pump AHA1 mutants,

supervised by Dmitry Yarmolinsky and Hannes Kollist.

2. I am aware of the fact that the author retains the rights specified in p. 1.

3. I certify that granting the non-exclusive licence does not infringe other persons' intellectual property rights or rights arising from the personal data protection legislation.

Jaanika Unt

11/06/2020